TARGETING THE TUMOR MICROENVIRONMENT WITH NANOPARTICLES FOR TREATMENT AND DIAGNOSTICS

Andreja Bratovš

Doctoral Dissertation
Jožef Stefan International Postgraduate School
Ljubljana, Slovenia

Supervisor: Prof. Dr. Olga Vasiljeva, Jožef Stefan Institute, Ljubljana, Slovenia
Co-Supervisor: Prof. DDr. Boris Turk, Jožef Stefan Institute, Ljubljana, Slovenia

Evaluation Board:
Prof. Dr. Marko Fonović, Chair, Jožef Stefan Institute, Ljubljana, Slovenia
Prof. Dr. Veronika Stoka, Member, Jožef Stefan Institute, Ljubljana, Slovenia
Prof. Dr. Ana Plemenitaš, Member, Faculty of Medicine, University of Ljubljana, Ljubljana, Slovenia

MEDNARODNA PODIPLOMSKA ŠOLA JOŽEFA STEFANA
JOŽEF STEFAN INTERNATIONAL POSTGRADUATE SCHOOL

Andreja Bratovš

TARGETING THE TUMOR MICROENVIRONMENT WITH NANOPARTICLES FOR TREATMENT AND DIAGNOSTICS

Doctoral Dissertation

TARČENJE TUMORSKEGA MIKROOKOLJA Z NANODELCI ZA ZDRAVLJENJE IN DIAGNOSTIKO

Doktorska disertacija

Supervisor: Prof. Dr. Olga Vasiljeva

Co-Supervisor: Prof. DDr. Boris Turk

Ljubljana, Slovenia, June 2020

Acknowledgments

I thank the Slovenian Research Agency for funding my doctoral studies.

I would like to thank my supervisor, Prof. Dr. Olga Vasiljeva, for the supervision of my dissertation, for the guidance and all the advice regarding my work. I am also thankful for the critical review of my doctoral thesis.

I would also like to thank my co-supervisor, Prof. DDr. Boris Turk, for accepting me into his research group, for ensuring good working conditions and for the advice regarding my work.

I would like to thank the members of my evaluation board, Prof. Dr. Marko Fonović, Prof. Dr. Veronika Stoka, and Prof. Dr. Ana Plemenitaš, for lending their expertise in the revision of my dissertation.

I would also like to thank Dr. Georgy Mikhaylov for all the help with designing and performing the experiments, as well as for his advice on presenting the results.

I am thankful to Dr. Lovro Kramer for his help and advice on my work.

I would like to thank all of the B1 Department for their help and advice, and for providing a stimulating work atmosphere.

Special thanks go to my family and friends for all their support during the course of the study.

Abstract

The tumor microenvironment (TME) is a complex system comprising various non-cancerous cell types and the extracellular matrix. Since tumor cells depend on the TME to sustain their growth and proliferation, targeting the cells and other components of the TME could provide an alternative or combination therapy. Targets in the TME include proteases, whose activity is one of the key elements supporting tumor development and metastasis, and the balance of intra- and extra- cellular concentrations of ions, which is an emerging area for cancer treatment. Here we applied nanotechnology, namely liposomes or aluminum nanoparticles for targeting cysteine proteases – cathepsins S and L – or disruption of the ion balance, respectively.

In the first part of our work, we have prepared a targeting system, based on liposomes, functionalized with an endogenous inhibitor of cysteine cathepsins – stefin A. The prepared system was tested *in vitro*, where it efficiently bound and inhibited cathepsins S and L. Application of stefin A-functionalized liposomes *in vivo* in a mouse model of breast cancer revealed its accumulation at the tumor site. Taken together, these results demonstrate a potential for cancer targeting for diagnostic and/or therapeutic approaches.

The second part of this work is focused on aluminum-based nanoparticles and their effect on cancer cells and the tumor microenvironment. Aloohene, an aluminum oxyhydroxide nanoparticle, does not owe its anti-tumor activity to either modulating the extracellular pH or damaging the lysosomes of cancer cells, however, it can cause significant ion imbalance in the cell perimembranous space through the selective adsorption of extracellular anions. Aloohene, θ- and γ-Al_2O_3 were shown to have a comparable effect on cancer cell lines viability and proliferation, therefore new types of nanoparticles with anti-tumor activity could be prepared using these forms of aluminum oxide.

Povzetek

Tumorsko mikrookolje je zapleten sistem, sestavljen iz nerakavih celic in zunajceličnega matriksa. Tumorskim celicam omogoča rast in delitev, zato bi lahko tarčenje celic in drugih delov tumorskega mikrookolja uporabili kot alternativne terapije za zdravljenje raka ali v kombinaciji z že obstoječimi terapijami. Tarče v tumorskem mikrookolju vključujejo proteaze, ki s svojo aktivnostjo pospešujejo razvoj tumorjev in metastaz, ter ravnovesje znotraj- in zunajceličnih ionskih koncentracij, ki je novo področje v razvoju terapij za zdravljenje raka. V našem delu smo uporabili nanotehnologijo, in sicer liposome in aluminijeve nanodelce, za tarčenje cisteinskih proteaz – katepsinov S in L – oz. za tarčenje ionskega ravnovesja.

V prvem delu naše raziskave smo pripravili sistem za tarčenje na osnovi liposomov, konjugiranih s stefinom A – endogenim inhibitorjem cisteinskih proteaz. Pripravljeni sistem smo preizkusili *in vitro*, kjer se je uspešno vezal na katepsina S in L ter inhibiral njuno aktivnost. Po aplikaciji liposomov s stefinom A v mišji model raka na dojki so se ti akumulirali na področju tumorja. Ti rezultati kažejo, da je sistem primeren za diagnostične in/ali terapevtske namene pri zdravljenju raka.

V drugem delu naše raziskave smo se posvetili nanodelcem na osnovi aluminija in njihovemu učinku na rakave celice ter tumorsko mikrookolje. Pokazali smo, da protitumorsko delovanje Aloohena, aluminijevega oksihidroksidnega nanodelca, ne temelji na spremembi zunajceličnega pH ali na povzročitvi lizosomskih poškodb v rakavih celicah. Zaradi visokega naboja bi lahko Aloohene povzročil znatne spremembe v ravnovesju ionov v perimembranskem prostoru, saj selektivno adsorbira zunajcelične anione. Pokazali smo tudi, da imajo Aloohene, θ- in γ-Al_2O_3 primerljiv učinek na viabilnost in delitev rakavih celičnih linij. Tako bi lahko θ- in γ-Al_2O_3 služila kot osnova za pripravo novih nanodelcev s protitumorskim delovanjem.

Contents

List of Figures

List of Tables

Abbreviations

ADC	. . . antibody-drug conjugate
AlOOH	. . . Aloohene
AMC	. . . 7-amino-4-methylcoumarin
APC	. . . antigen presenting cell
BrdU	. . . 5-bromo-2'-deoxyuridine
BSA	. . . bovine serum albumin
CAF	. . . cancer-associated fibroblasts
CT	. . . computer tomography
DARPin	. . . designed ankyrin repeat protein
DiR'	. . . 1,1'-dioctadecyl-3,3,3',3'-tetramethylindotricarbocyanine iodide
DiR'-LP	. . . DiR'-containing liposomes
DLS	. . . dynamic light scattering
DMSO	. . . dimethyl sulfoxide
DNA	. . . deoxyribonucleic acid
DTT	. . . dithiothreitol
ECM	. . . extracellular matrix
EDTA	. . . ethylenediaminetetraacetic acid
EPR	. . . enhanced permeability and retention
GAG	. . . glycosaminoglycan
HRP	. . . horseradish peroxidase
IONP	. . . iron oxide nanoparticles
JAM	. . . junctional adhesion molecule
K_i	. . . inhibition constant
LP	. . . liposomes
M6PR	. . . mannose-6-phosphate receptor
MDSC	. . . myeloid-derived suppressor cells
MMP	. . . matrix metalloprotease
MRI	. . . magnetic resonance imaging
MTT	. . . 3-(4,5-dimethylthiazol-2-yl)-2,5-diphenyltetrazolium bromide
NK	. . . natural killer
NLC	. . . nanostructured lipid carriers
OT	. . . orthotopical
PBS	. . . phosphate-buffered saline
PEG	. . . polyethylene glycol
PyMT	. . . polyoma middle T antigen
Rho	. . . PE lissamine rhodamine B
Rho-LP	. . . liposomes containing rhodamine
RNA	. . . ribonucleic acid
SDS-PAGE	. . . sodium dodecyl sulfate-polyacrylamide gel electrophoresis
SLN	. . . solid lipid nanoparticles
StA-DiR'-LP	. . . stefin A[D61C]-conjugated liposomes containing DiR′

StA-LP	... stefin A[D61C]-conjugated liposomes
StA-Rho-LP	... stefin A[D61C]-conjugated liposomes containing rhodamine
TAM	... tumor-associated macrophage
TME	... tumor microenvironment

Standard Amino Acid Abbreviations

Amino acid	Three-letter abbreviation	One-letter abbreviation
Alanine	Ala	A
Arginine	Arg	R
Asparagine	Asn	N
Aspartic acid	Asp	D
Cysteine	Cys	C
Phenylalanine	Phe	F
Glycine	Gly	G
Glutamine	Gln	Q
Glutamic acid	Glu	E
Histidine	His	H
Isoleucine	Ile	I
Leucine	Leu	L
Lysine	Lys	K
Methionine	Met	M
Proline	Pro	P
Serine	Ser	S
Tyrosine	Tyr	Y
Threonine	Thr	T
Tryptophan	Trp	W
Valine	Val	V

Chapter 1

Introduction

1.1 Cancer

Cancer is the second leading cause of mortality worldwide, next to cardiovascular diseases. In 2018, more than 9 million people died of cancer, while more than 18 million new cases were diagnosed (WHO, 2018). Breast cancer is among the most prevalent types of cancer, next to lung and colon cancer, while being the leading type of cancer in women (WHO, 2018).

The fundamental abnormality leading to the development of cancer is the continued and unregulated proliferation of cancer cells, which leads to the formation of tumors. The cause for the transformation of normal cells to cancer cells is their genetic instability, which can arise from radiation exposure, hormonal instability, toxic chemicals, microbial infection or a hereditary genetic mutation. Through mutations, cancer cells become unresponsive to anti-growth signals that maintain homeostasis within normal tissue, while also becoming self-sufficient in growth signals. Furthermore, they escape cell death through the loss of proapoptotic proteins and upregulation of antiapoptotic genes. Through the abnormal activity of telomerase, cancer cells are able to maintain telomere length above a critical threshold, thus acquiring limitless replicative potential. Moreover, they are capable of sustained angiogenesis, tissue invasion and metastasis (Hanahan & Weinberg, 2000, 2011). During tumor progression, malignant cells first invade the surrounding tissue and later distant body sites through dissemination and metastasis (Cooper & Hausman, 2000).

In addition to mutations, inflammation also contributes to acquiring many of the above-mentioned cancer hallmarks. The role of inflammation in tumor progression is dichotomous; immune cells exhibit a tumor-suppressing activity and destroy the newly formed cancer cells. However, the chronic inflammatory response enhances tumorigenesis and progression by providing bioactive molecules, such as growth factors, proangiogenic factors or extracellular matrix remodeling enzymes, which facilitate invasion and metastasis. Chronic inflammation correlates with cancer progression in almost all solid tumors, and in some cases, inflammation can be the cause of tumor formation. The most frequent cancers caused by inflammation are stomach cancer, which arises from infection by *Helicobacter pylori* and colorectal cancer following an inflammatory bowel disease (Shalapour & Karin, 2015).

1.1.1 Tumor microenvironment

Tumor microenvironment (TME) is a complex system comprising various non-cancerous cell types and the extracellular matrix (Figure 1). Immune response and inflammation play an important role in cancer development and accordingly, a large part of the cells in the TME are different types of immune cells, such as tumor-associated macrophages, regulatory

T cells, myeloid-derived suppressor cells, neutrophils, dendritic cells, and natural killer cells (Balkwill, Capasso, & Hagemann, 2012).

Tumor-associated macrophages (TAMs) are important regulators of tumorigenesis, supporting multiple aspects of tumor progression, and are a major source of proteases in the TME (Joyce et al., 2004; Quail & Joyce, 2013). They are abundant in most human and experimental murine cancers and are associated with malignant cell migration, invasion, and metastasis (Condeelis & Pollard, 2006). Furthermore, TAMs contribute greatly to tumor angiogenesis (Lin et al., 2006). Macrophages are functionally plastic, which enables them to alter their polarization depending on physiological conditions to either "classically activated" M1 state or the "alternatively activated" M2 state, to which they are driven in the TME (Mosser & Edwards, 2008). M2 macrophages produce type II cytokines, promote anti-inflammatory responses, and have pro-tumorigenic functions. Major factors in the conversion of macrophages to TAMs are microenvironment conditions, such as hypoxia (Balkwill et al., 2012; Quail & Joyce, 2013).

In addition to protumorigenic immune cell types, some tumor-suppressing immune cell types are also present in the TME, such as some B and T lymphocytes and natural killer (NK) cells. Even though their abundance usually correlates with better prognosis in cancer (Coronella et al., 2001; Tachibana et al., 2005), these cells can be inhibited by the tumor-promoting cell types, such as myeloid-derived suppressor cells (MDSCs). Their immunosuppressive activity helps maintain normal tissue homeostasis; however, it can also enable tumor cells to evade the immune system. MDSCs are mobilized during tumorigenesis and infiltrate developing tumors (Talmadge & Gabrilovich, 2013). They promote tumor progression by disrupting mechanisms of immunosurveillance, such as antigen presentation by dendritic cells, T cell activation, NK cell cytotoxicity and M1 macrophage polarization (Balkwill et al., 2012; Quail & Joyce, 2013). PD-1/PD-L1 pathway also plays an important role in cancer immunosuppression. Programmed cell death protein 1 (PD-1) promotes self-tolerance through suppressing the activity of T lymphocytes, thus protecting against autoimmunity. After PD-1 binds to its ligand (PD-L1 or PD-L2), several signaling pathways are either activated or inhibited and the accumulative effect on the T cell diminishes its proliferation and promotes loss of its effector functions. Tumor cells and tumor-associated immune cells can also exploit the PD-1/PD-L system by expression of PD-L1 or PD-L2. Several antibodies blocking the PD-1/PD-L1 pathway are now approved for multiple indications or in clinical trials.

Non-immune cells also play an important role in the TME. Cancer-associated fibroblasts (CAFs) represent a different cell type than normal fibroblasts and can be derived from several different precursors during disease progression (Marsh, Pietras, & McAllister, 2013). Once accumulated in the TME and activated by growth factors and cytokines, CAFs are a major source of secreted tumor-promoting growth factors and pro-inflammatory factors (Erez, Truitt, Olson, Arron, & Hanahan, 2010; Quail & Joyce, 2013).

As mentioned above, angiogenesis is one of the hallmarks of cancer and the TME promoting tumor vasculature. Tumor vascularization requires the collaboration of different types of cells in the TME, including vascular endothelial cells and pericytes as well as TAMs and CAFs (Semenza, 2013). Tumor vasculature is abnormal in its structure and function; the blood vessels are chaotically branched and leaky. This causes uneven oxygenation, which increases hypoxia facilitating metastasis (Jain, 2005).

The extracellular matrix (ECM) is another key component of the TME. Surrounding the cells, it is composed of many types of macromolecules, such as collagen, laminin, fibronectin, and heparin sulfate proteoglycans, which link together and form a 3D matrix. Several families of matrix-degrading enzymes, including proteases from cysteine, serine and matrix metalloprotease (MMP) classes, mediate ECM remodeling. In the TME, controlled

ECM degradation is necessary for angiogenesis and tumor invasion. The ECM is also a rich source of progrowth and proangiogenic factors (Balkwill et al., 2012).

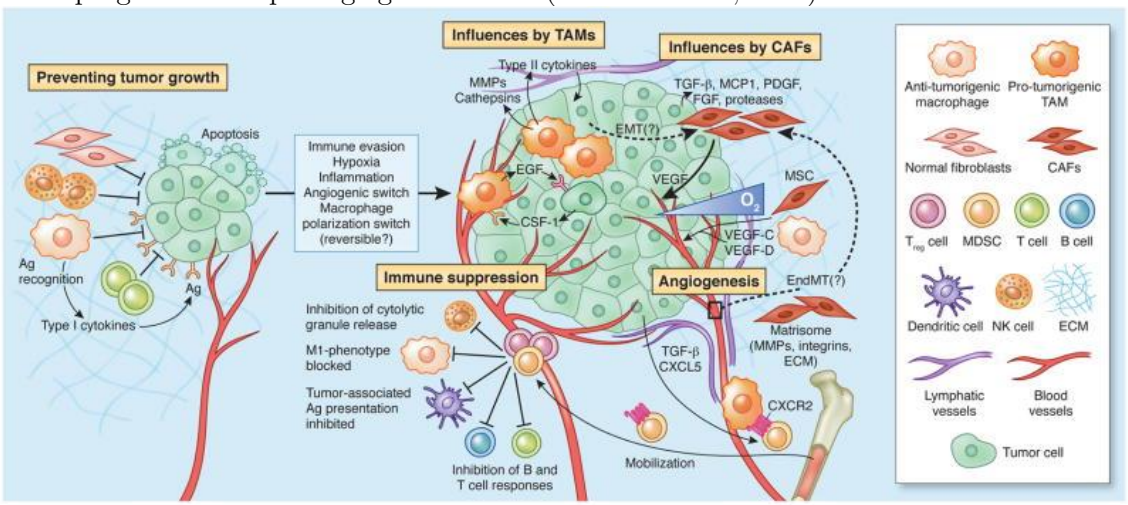

Figure 1: Stromal cells support tumor growth and progression (Quail & Joyce, 2013).

1.1.1.1 Targeting the tumor microenvironment

Therapeutic approaches to treat cancer rely on targeting tumor cells. Since tumor cells depend on the TME to sustain their growth and proliferation, targeting the cells and other components of the TME could provide an alternative or combination therapy. Additionally, the non-cancerous cells of the TME are genetically stable and thus less prone to develop drug resistance. However, there is a balance between the tumor-inhibitory and tumor-promoting functions of the cells in the TME; therefore, the targets for such therapeutics must be carefully selected (Joyce, 2005).

Blocking the activity of ECM degrading enzymes is a promising strategy since it offers the potential to inhibit tumor invasion as well as limit the access of tumor cells to growth factors. However, some matrix-degrading enzymes, such as MMPs, can also release antiangiogenic factors, which inhibit tumorigenesis (Hamano et al., 2003). Blocking their activity could have side effects as was shown for the broad-spectrum MMP inhibitors (Coussens, Fingleton, & Matrisian, 2002). Targets among the matrix-remodeling enzymes should, therefore, be selected with caution.

Integrins, a family of heterodimeric receptors, are another target in the extracellular matrix. They connect cells to the ECM, are upregulated in cancer, and expressed on the tumor cell surface. Blocking their functions should interfere with angiogenesis, cell survival, cell adhesion, and motility. Antibodies, which disrupt the binding of some integrins are already in the clinical trials. Examples include Vitaxin, whose target is integrin $\alpha v\beta 3$ and Volociximab, targeting integrin $\alpha 5\beta 1$ (Hood & Cheresh, 2002; Jin & Varner, 2004).

Since it has been established that tumors cannot grow without their own blood supply, targeting tumor vasculature is a promising approach and the development of therapeutics ranges from a plethora of antiangiogenic agents that inhibit angiogenic factors or their receptors (Papetti & Herman, 2002), to targeting pericytes and endothelial progenitor cells (Joyce, 2005).

Considering the important role of chronic inflammation in cancer, anti-inflammatory drugs targeting proinflammatory factors such as COX-2, IkB kinase, TNFα and some of the interleukins, are also being tested in clinical trials as cancer therapeutics (Joyce, 2005). An alternative strategy could be to target factors released by immune cells in the TME

specifically, including urokinase plasminogen activator receptor, cathepsins, and heparanase (Dranoff, 2004).

Antibody-drug conjugates (ADCs) have been used for more than twenty years as a tool to deliver cytotoxic agents directly to the tumor site. While efforts were mainly focused on the development of internalizing ADCs, there are also some advantages of preparing non-internalizing ADC products that release their cargo into the TME, allowing the drug to reach cancer cells by passive diffusion, thus targeting also the antigen-negative cancerous cells (Lambert, 2013).

Recently, the cell membrane potential and the equilibrium of extracellular and intracellular ion concentrations in cancer cells have become a research interest, and their disturbance is a promising strategy for new anticancer drugs (Brisson et al., 2011; Yildirim, Altun, Gumushan, Patel, & Djamgoz, 2012).

1.2 Cysteine Cathepsins and Their Protein Inhibitors

1.2.1 Cysteine cathepsins

Cysteine cathepsins are a group of lysosomal proteases from the C1 family of papain-like enzymes. There are 11 human cysteine cathepsins: cathepsins B, C, F, H, K, L, O S, V, X, and W. They are optimally active in a reducing, slightly acidic environment, such as the lysosome, and their role was initially considered as limited to non-specific, bulk proteolysis in the endolysosomal compartments. This view has changed in the last years, as more specialized roles began to emerge, such as the role of cathepsin K in bone remodeling and cathepsin S in antigen presentation (V. Turk et al., 2012).

Cysteine cathepsins are synthesized as preproenzymes on the endoplasmic reticulum, where the signal peptide is also cleaved and N-glycosylation occurs. They are trafficked to the endolysosomes via the mannose-6-phosphate receptor (M6PR). In the mildly acidic environment of the endosome, cathepsins dissociate from the M6PR and can be activated by the cleavage of the propeptide, which occurs autocatalytically or by another protease. Although cathepsins were traditionally seen as intracellular lysosomal enzymes, many physiological and pathological scenarios where they are secreted are now known (V. Turk et al., 2012).

The 3D structure of cysteine cathepsins is highly conserved – they all exhibit the papain fold (Guncar, Pungercic, Klemencic, Turk, & Turk, 1999). They are composed of two domains: the left (L-) and the right (R-) domain (Figure 2). The domains form a cleft in the middle of the structure, where the active site is located. The active site cysteine is part of the L-domain and the active site histidine is located on the R-domain. The two catalytic amino acid residues form the thiolate-imidazolium ion pair, which is essential for the protease activity. Most of the cysteine cathepsins are endopeptidases, except for cathepsins H and B, which exhibit aminopeptidase and carboxypeptidase activity, respectively, in addition to the endopeptidase activity, and cathepsins X and C, which are exopeptidases only. In the endopeptidases, substrates bind to the active-side cleft, which extends along the whole length of the two-domain interface. Cysteine cathepsins have a broad specificity, cleaving preferentially after basic or hydrophobic residues (V. Turk et al., 2012).

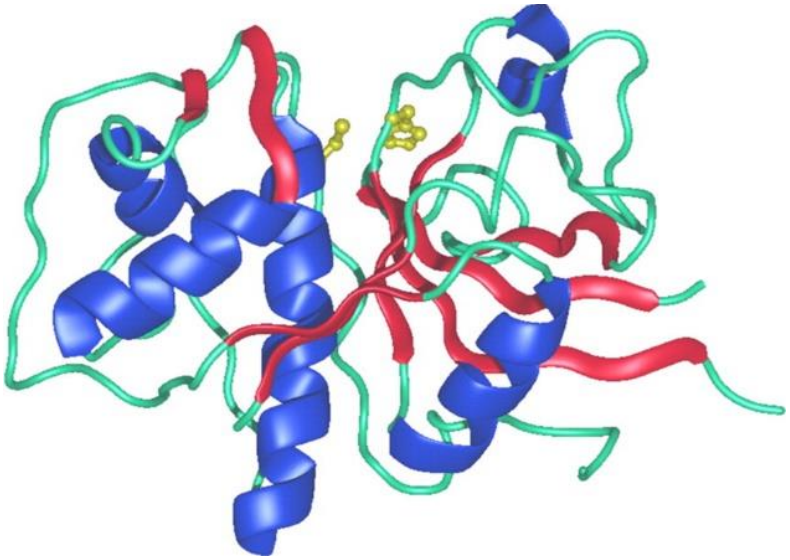

Figure 2: The structure of cathepsin L with the active site residues colored in yellow (V. Turk et al., 2012).

The classical physiological role of cathepsins is bulk proteolysis of proteins in the lysosomes; however, some of the specific physiological roles take place outside of lysosomes. One of the more researched aspects of cathepsins is their involvement in adaptive immunity, where they are crucial for the processing of invariant chain and additionally generate peptides, which are presented to MCH class-II molecules (Nakagawa et al., 1998). A number of cathepsins participate in bone remodeling and resorption. While only cathepsin K can cleave collagen, several of the cathepsins cleave gelatin, its partially degraded form (Z. Li, Hou, Escalante-Torres, Gelb, & Bromme, 2002). Cathepsins also release glycosaminoglycans (GAGs) from cartilage proteins such as aggrecan. In addition to being released by cathepsins, GAGs play a crucial role in the formation of complexes between cysteine cathepsins and their protein substrates and have been shown to regulate their activity (Z. Li et al., 2004). Another non-classical role of cathepsins is the processing of thyroglobulin, followed by hormone release (Jordans et al., 2009). Cathepsins were also shown to be involved in the modulation of T-cell migration, which is achieved by targeting integrins (Obermajer et al., 2008).

Cysteine cathepsins have also been shown to play an important role in many inflammatory diseases, including cancer. Their expression is upregulated in many types of cancer and they were demonstrated to contribute to different stages of cancer progression.

1.2.1.1 Structural and functional properties of cathepsins L and S

Cathepsin L is an endopeptidase, ubiquitously expressed in tissue. It is catalytically active from pH 3 to pH 6.5 in the presence of thiol compounds. The preproenzyme form of cathepsin L is composed of 333 amino acid residues with a molecular mass of 38 kDa. On SDS-PAGE, additional forms were determined: single-chain form at 28 kDa, heavy chain at 24 kDa and light chain at 4 kDa. Activation of cathepsin L occurs autocatalytically or by the action of cathepsin D or metalloendopeptidases (Menard et al., 1998; Nishimura, Kawabata, Furuno, & Kato, 1989). One of the main biological functions of cathepsin L is proteolysis in lysosomes; this results not only in protein degradation, but also generates specific antigenic peptide repertoire for the MHC class II cells (Honey et al., 2002; Hsieh, deRoos, Honey, Beers, & Rudensky, 2002). Cathepsin L also regulates the recycling of growth factor EGF and growth factor receptors (Reinheckel et al., 2005). Cathepsin L has

been found in the nucleus, where it can play a role in the regulation of the cell cycle progression by the degradation of transcription factors (Reinheckel et al., 2005).

Cathepsin S is also an endopeptidase, predominantly expressed in the professional antigen-presenting cells (APCs). In contrast to other cysteine cathepsins, cathepsin S is stable and active at neutral pH, with the pH optimum at pH 6.5. Similarly to cathepsin L, cathepsin S is synthesized as a preproenzyme of 331 amino acid residues with a molar mass of 37 kDa. The mature form of cathepsin S is a single-chain polypeptide, 24 kDa in size. Procathepsin S can be autocatalytically activated at pH 4.5 (Beers et al., 2005). The most important biological role of cathepsin S, in addition to proteolysis in lysosomes, is in the immune response. Cathepsin S is crucial for the processing of invariant chain in APCs and antigen presentation (Beers et al., 2005).

1.2.1.2 The roles of cathepsins L and S in cancer

Cysteine cathepsins have been shown to play an important role in cancer progression and are overexpressed in many cancer types. They are also secreted into the TME, either by tumor cells, which is the case for cathepsin L, or by immune cells, which are the major source for secreted cathepsin S (Kramer, Turk, & Turk, 2017).

Both cathepsin L and S were found to be upregulated in colorectal cancer (Adenis et al., 1995; Gormley et al., 2011), lung cancer (Kos et al., 2001; Ledakis et al., 1996) and glioma (Kenig, Alonso, Mueller, & Lah, 2010; Strojnik, Kavalar, Trinkaus, & Lah, 2005), while cathepsin L is also upregulated in pancreatic cancer (Niedergethmann et al., 2004) and breast cancer (Lah et al., 1992; Thomssen et al., 1995). In most cases, high cathepsin L or S expression is associated with poor prognosis, poor response to therapy or linked with metastasis (Olson & Joyce, 2015). However, the role of cathepsin L is contradictory, as it can either enhance or inhibit carcinogenesis, depending on the context. In the RIP1-Tag2 mouse model of pancreatic cancer, ablation of cathepsin L lowers tumor burden (Gocheva et al., 2006). In contrast, the opposite effect is observed in mouse models of skin carcinoma, where loss of cathepsin L enhances carcinogenesis (Benavides et al., 2012).

In the TME, cathepsins L and S are implicated in the regulation of tumor angiogenesis. They can stimulate angiogenesis directly by generating pro-angiogenic factors or indirectly by regulating pro-angiogenic proteolytic networks (Veillard et al., 2011; B. Wang et al., 2006). Another important contribution of cysteine cathepsins, including cathepsins S and L, to the TME, is the degradation of ECM and the establishment of invasion tracks (Guinec, Dalet-Fumeron, & Pagano, 1993). Additionally, they also cleave specific cell-cell adhesion molecules, such as E-cadherin, which has been identified as a substrate for cathepsins S and L in RIP1-Tag2 tumors (Gocheva et al., 2006). Furthermore, cathepsin S mediates the cleavage of several junctional adhesion molecules (JAMs), which allows cancer cells to breach the blood-brain barrier (Sevenich et al., 2014).

Cysteine cathepsins were also shown to contribute to the therapeutic resistance of tumors. Cathepsin S was demonstrated to have a role in cancer cell resistance to ionizing radiation (H. J. Lee et al., 2008). Cathepsin S, along with cathepsin B, was also shown to be a key mediator in the chemoprotective effect of macrophages, where TAMs protect breast cancer cells from chemotherapy-induced cell death (Shree et al., 2011).

1.2.2 Cystatins

Cystatins are a group of endogenous protein inhibitors of cysteine cathepsins. They are competitive, tight-binding inhibitors and they act as emergency inhibitors, meaning they are usually separated from their target enzymes and act on escaped proteases or proteases

of invading pathogens. Based on the presence and number of disulfide bonds and the number of cystatin-like domains, cystatins are divided into three inhibitor types, namely stefins, cystatins and kininogens, and a group of non-inhibitory homologs (Vito Turk & Bode, 1994; V. Turk et al., 2012).

1.2.2.1 Stefin A

Stefin A, belonging to the stefins group of cathepsins inhibitors, is a single-chain intracellular protein of 98 amino acid residues with a molar mass of 11 kDa. It is highly thermostable with the transition temperature for thermal denaturation at 94.5 °C and lacks disulfide bonds. The structure of stefin A consists of a five-stranded β-sheet and one α-helix, which form a cystatin fold (Figure 3). The N-terminal region and two hairpin loops form a wedge, which binds into the active-site cleft of the enzyme and prevents substrate binding. The first loop with the amino acid sequence QVVAG is crucial for binding to the protease (Jenko et al., 2003; Renko, Pozgan, Majera, & Turk, 2010). Other important residues include Gly4 on the N-terminal tail and residues Leu73 and Pro74 on the second loop (Estrada et al., 1998; Pavlova & Bjork, 2002).

Stefin A inhibits cathepsin S, L, and H with the inhibition constant in the picomolar range, while its affinity for cathepsin B is lower. It also inhibits parasitic proteases, such as cruzipain, and plant proteases, such as papain and actinidin (V. Turk et al., 2012).

Its features, namely small molecular size, absence of post-translational modifications and disulfide bonds, high thermostability and the fact that the recombinant protein is easily prepared, make stefin A very suitable for use in protein engineering. It has already been used as a scaffold for peptide aptamer presentation. By mutating crucial amino acid residues, the cathepsins binding site was removed. The loops were then replaced with aptamers, which enable selection for specificity for a target protein (Hoffmann et al., 2010).

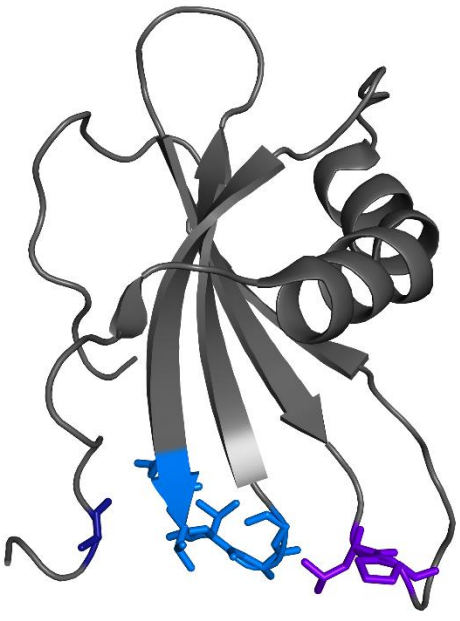

Figure 3: Stefin A structure with enzyme interacting residues colored and shown as sticks: Gly4 (dark blue), QVVAG loop (light blue), Leu73 and Pro74 (purple) (PDB ID: 3KM9).

1.3 Nanoparticles in Cancer Diagnostics and Treatment

Nanotechnology is an emerging tool for cancer diagnosis and therapy, where nanoparticles can be used to induce cell toxicity, or as drug delivery systems, improving the bioavailability of the drug and, thus, reducing side effects. Nanoparticles are particles in dimensions of roughly 1-100 nm. Nanomaterials utilized in cancer drug design and delivery vary in their composition and physicochemical properties, such as size, shape and surface characteristics. They can be roughly grouped into the following types: lipid-based nanocarriers, polymer-based nanocarriers, inorganic nanoparticles, viral nanoparticles and drug conjugates (Figure 4) (Tran, DeGiovanni, Piel, & Rai, 2017).

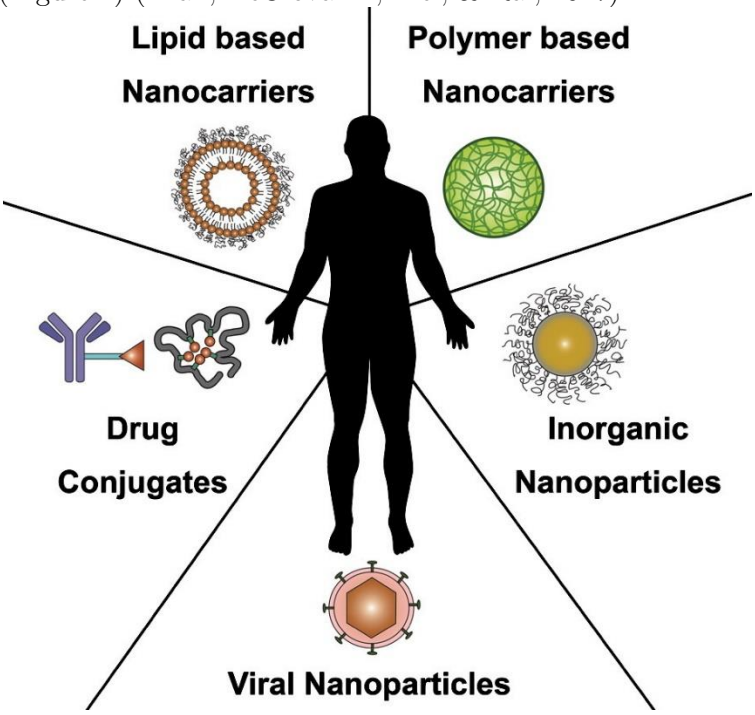

Figure 4: Schematic illustration of established nanotherapeutic platforms (Tran et al., 2017).

Liposomes, the spherical phospholipid bilayer nanoparticles, are the most widely used lipid-based nanocarriers, but some research was also done on the lipid monolayer micelles. New forms of nanocarriers using lipids other than phospholipids are also being developed, such as solid lipid nanoparticles (SLNs) and nanostructured lipid carriers (NLCs). The SLNs are composed of a solid lipid core in the form of crystal lipid matrices that can accommodate the loaded drug. In contrast, the NLC have an amorphous lipid core, which shows enhanced drug loading (Puri et al., 2009).

Polymer nanocarriers can be based on natural or synthetic polymers. Natural polymers used in nanotechnology include peptides and proteins, among which the only clinically used protein nanocarrier is albumin-nanoparticle-bound paclitaxel, and glycans, such as cyclodextran and chitosan. Synthetic polymer-based nanocarriers are more chemically versatile and a number of them are in clinical tests. Examples include PEG-PGA polymeric micelles for the delivery of cisplatin, PLGA-PEG nanoparticles encapsulating docetaxel and poly(amidoamine) dendrimers for the delivery of short-activating RNA (Wicki, Witzigmann, Balasubramanian, & Huwyler, 2015).

Drug conjugates are also classified as nanoparticles because of their size scale. They are the most successful nanomedicine therapeutics in clinical cancer care. In contrast to other

nanocarriers, where the drug is encapsulated, in drug conjugates, active agents are covalently linked to targeted antibodies, peptides or polymers. Antibody drug conjugates approved for clinical use include trastuzumab-emtasine against HER2 in breast cancer and brentuximab-vedotin against CD30 in non-Hodgkin lymphoma (Tran et al., 2017; Wicki et al., 2015).

Inorganic nanoparticles can be metallic – based on metals or metal oxides, or non-metallic. Non-metallic inorganic nanoparticles include mesoporous silica nanoparticles and carbon nanotubes. Most of the research on metallic nanoparticles focuses on gold, silver and iron nanoparticles (Bayda et al., 2018).

Another way to construct nanoparticles is to use tumor-homing viruses, which are engineered to express therapeutic proteins. Specific features of cancer cells, such as blocked apoptosis pathways, deregulation of cell replication and immune evasion, are also beneficial for viral replication. Examples of viral nanoparticles in clinical trials include JX-594, a poxvirus designed to kill tumor cells via activation of the EGFR-Ras-MAPK pathway, tested on liver cancer patients (Wicki et al., 2015).

1.3.1 Liposomes

Liposomes were the first nanotechnology used in cancer treatment. The liposomal structure was described in 1964 and the first liposomal therapeutic – the liposome-encapsulated doxorubicin or Doxil, was approved by the FDA in 1995 (Barenholz, 2012).

Liposomes are spherical self-forming structures with a single phospholipid bilayer, typically 25-100 nm in size. A variety of phospholipids can be used to prepare liposomes; among the most common are distearoyl (with a saturated hydrocarbon chain) and dioleoyl phosphatidylcholine (with an unsaturated hydrocarbon chain). Liposomes owe their success as a drug delivery agent to their ability to protect encapsulated drugs from degradation and to improve the biodistribution of drugs. They can be loaded with water-soluble molecules in their aqueous core or with lipophilic drugs in the lipid bilayer. To improve circulation times of liposomes and to reduce their uptake by the macrophages, liposomes were coated with PEG. PEG forms a water-retaining coat around the liposome and prevents recognition by the reticuloendothelial system. Such PEGylated liposomes were termed “stealth liposomes” (Allen & Cullis, 2013). To target liposomes to the tumor, various strategies were implemented, including passive and active targeting.

1.3.1.1 Passive targeting

The tumor-associated blood vessels are leaky; the size of gaps between the endothelial cells ranges from 100 to 780 nm, as opposed to 5-10 nm in normal endothelium. Additionally, solid tumors lack adequate lymphatic drainage. This results in the accumulation of macromolecules and nanoparticles in the TME. This well-established phenomenon has been termed the enhanced permeability and retention effect (EPR) (Greish, 2010). Liposomes, as well as other nanoparticles, are passively targeted to tumor tissue due to the EPR effect (Ngoune, Peters, von Elverfeldt, Winkler, & Putz, 2016). Furthermore, owing to the PEG coating, liposomes have a longer circulation time and the higher number of passages through the tissue enhances the EPR effect (Allen, Hansen, Martin, Redemann, & Yau-Young, 1991).

In order to utilize the EPR effect, liposomes need to be of an appropriate size; effective extravasation has been shown for particles smaller than 200 nm (Danhier, Feron, & Preat, 2010). Other factors influencing passive targeting are the composition and surface charge of liposomes. Cationic liposomes tend to localize in tumor vessels, however, they also non-

specifically interact with anionic molecules in the blood, leading to their clearance from circulation (Zhao, Zhuang, & Qi, 2011).

1.3.1.2 Active targeting

The aim of actively targeted liposomes is to minimize off-target effects. Active targeting is achieved by functionalizing the liposomal surface with targeting moieties, which include small-molecule ligands, peptides, and monoclonal antibodies. Targets to be considered for active targeting need to be specific for tumor cells. They can be either highly overexpressed in tumor cells or differentially located compared to healthy cells. Another requirement for targets is that they are present extracellularly (Byrne, Betancourt, & Brannon-Peppas, 2008).

One group of targets exploited for active targeting are cancer cell surface receptors. Many cell surface receptors are highly upregulated in tumor cells. Their localization on the cell membrane makes them available for binding by liposomes. Once bound to the targeting receptor, liposomes could be internalized thus delivering the toxic payload to the cell. Targeting agents used to target receptors include ligands, specific for the receptor, as is the case for the folate receptor and the transferrin receptor (X. Li, Ding, Xu, Wang, & Ping, 2009; Watanabe, Kaneko, & Maitani, 2012). Alternatively, antibodies against the receptors can be used and this strategy was employed for targeting EGFR and HER-2 receptors (Kim & Huang, 2012; Shmeeda, Tzemach, Mak, & Gabizon, 2009). Antibody-functionalized liposomes are also termed immunoliposomes (Paszko & Senge, 2012).

The molecules in the TME can also be used for active targeting to the tumor. Targets in the TME include VEGF (Katanasaka, Ida, Asai, Maeda, & Oku, 2008), VCAM (Gosk, Moos, Gottstein, & Bendas, 2008) and integrins (Du, Cui, Wang, Liu, & Cui, 2011). Proteases acting on the EMC, such as MMPs (Hatakeyama et al., 2007) and cathepsins (Mikhaylov et al., 2014), have also been targeted.

A different approach has also been used in targeted drug delivery: utilizing local stimuli to achieve enhanced drug release. Based on the characteristics specific to the tumor microenvironment, liposomes that release their cargo when they enter the tumor have been developed. In the TME, pH is slightly acidic and pH-sensitive liposomes have been designed to enable pH-triggered drug delivery (Koren, Apte, Jani, & Torchilin, 2012). Similarly, temperature- and redox- triggered liposomes have also been prepared, exploiting the fact that inflamed tissues, such as tumors, show hyperthermia, and that the redox potential is higher in tumor tissues (Goldenbogen et al., 2011; Grull & Langereis, 2012). Enzymes specific for the TME have been utilized as triggers to either cleave and disrupt the liposomes, thus releasing their cargo, or to cut a linker and reveal a hidden functionality (Banerjee et al., 2009).

1.3.1.3 Multifunctional liposomes

More recently, drug delivery systems with more than one useful attribute have been developed. Liposomes are a convenient platform in such designs, since their surface can be functionalized with multiple moieties in addition to the encapsulation of the active substance. Multifunctional liposomes can combine several of the following properties: they specifically target the tumor, respond to local stimuli and carry an imaging agent to enable their detection. The last property opens the possibilities to use liposomes in the theranostics field – simultaneously achieving diagnostics and therapy (Deshpande, Biswas, & Torchilin, 2013; Gindy & Prud'homme, 2009; Torchilin, 2009).

1.3.2 Metallic nanoparticles

Metallic nanoparticles are based on metals or their oxides. Their shell can also be organic to stabilize the particle and provide functionalization. Metallic nanoparticles show some unique properties, including large surface area-to-volume, ease of synthesis, and the possibility of surface modification, which make them promising for the use in cancer nanomedicine. They can be used as a delivery system or as a diagnostic tool or can have cytotoxic properties (Bayda et al., 2018).

One of the strategies to use metallic nanoparticles for cancer treatment is photothermal therapy, where the nanoparticles are stimulated with a near-infrared laser. The absorbed energy is then released as heat and ablates the surrounding cancer cells. Gold nanoparticles are especially suited for this therapy due to their high absorption in the near-infrared region (Mayle et al., 2017). A similar approach is possible with magnetic iron oxide nanoparticles (IONPs), which produce hyperthermia due to localized heating in a magnetic field (Hilger et al., 2002). Magnetic IONPs have an additional benefit – the possibility to target them to the tumor site with a magnet (Mikhaylov et al., 2011).

Silver is well known for its antimicrobial properties and has been a gold standard in the antibacterial treatment of serious burn wounds (Klasen, 2000). Similarly, silver nanoparticles have been used for wound management. Furthermore, silver nanoparticles have also shown promising anti-cancer effects. *In vitro*, they have lowered the viability of acute myeloid leukemia cells and human breast cancer cells through the generation of reactive oxygen species and release of silver ions, which stimulate DNA damage and apoptosis (Guo et al., 2014; Gurunathan, Han, Eppakayala, Jeyaraj, & Kim, 2013).

Therapeutic agents can be conjugated to the metallic nanoparticles, transforming them into drug delivery systems. TNFα has been conjugated to colloidal gold nanoparticles and is currently in clinical trials for the treatment of non-small lung cancer. IONPs also have the potential to incorporate therapeutics (Goel, Shah, Visaria, Paciotti, & Bischof, 2009; Libutti et al., 2010).

Most of the clinically approved metallic nanoparticles are used in diagnostics since their special physicochemical characteristics make them very useful in imaging. Gold nanoparticles have been researched as CT contrast agents, while gadolinium nanoparticles and several types of IONPs are promising MRI agents (Bayda et al., 2018; Mikhaylov et al., 2011).

1.3.2.1 Aluminum-based nanoparticles

Aluminum is the most abundant metal in the Earth's crust, but it has no known biological function. In medicine, aluminum has been used as an adjuvant in vaccines for over six decades and its safety has been well established (Golos & Lutynska, 2015).

Aluminum oxide or alumina is a low-cost material, used in various domains, including biomedical applications. Alumina occurs in two forms, corundum and transition aluminas, differing in packing of oxygen atoms. Transition alumina is prepared from aluminum hydroxides. Aluminum oxyhydroxide or boehmite is a layered aluminum oxide hydroxide with an ordered laminated structure composed of parallel double chains of AlO_6 octahedra held together by the relatively weak hydrogen bonds. Boehmite is an important precursor from which various transition alumina, including θ- and γ-Al_2O_3, can be prepared. Different types of boehmite and alumina differ in particle size, specific surface area, and crystallinity (Alphonse & Courty, 2005).

Recently, a novel nanomaterial composed of agglomerated radially assembled Al hydroxide crumpled nanosheets was developed and termed Aloohene. Aloohene has

exhibited potent antitumor activity in murine cancer models due to its high specific surface area, positive charge and selective adsorption properties (Lerner et al., 2018).

Chapter 2

Purpose of the Work

The purpose of this dissertation is to develop novel cancer treatment approaches:

1. A drug delivery system based on liposomes targeting cathepsins S and L, highly upregulated proteases in TME. We will assemble and test the system utilizing their specific inhibitor, both *in vitro* and *in vivo*, to confirm the successful targeting of the tumor.
2. Disruption of extracellular ion balance of tumor cells by the use of aluminum hydroxide nanoparticles (Aloohene). We will investigate their effect on cell lines in terms of their viability, lysosomal damage, and extracellular pH. We will also test the cytotoxic activity of some similar nanoparticles.

The hypotheses of this research were the following:

1. Stefin A [D61C]-conjugated liposomes bind to and inhibit recombinant cathepsins S and L. Stefin A [D61C]-conjugated liposomes accumulate better in tumors compared to non-conjugated liposomes.
2. We expect that Aloohene has the most effect on cell lines viability, compared to other aluminium-based nanoparticles. We do not expect Aloohene to affect lysosomal permeability or extracellular pH.

The main goals of the research were:

1. Developing stefin A-conjugated liposomes as a targeted drug delivery system:
    - preparation and characterization of stefin A-conjugated liposomes,
    - determination of stefin A-conjugated liposomes binding and inhibition of recombinant cathepsin S and L *in vitro*,
    - validation of stefin A-conjugated liposomes localization *in vivo* using a murine breast cancer model.
2. Investigating the effect of aluminum-based nanoparticles on cells and their environment:
    - evaluation of the effect of different aluminum-based nanoparticles on cell lines viability,
    - determination of Aloohene nanoparticles' effect on lysosomal permeability and extracellular pH.

Chapter 3

Materials and Methods

3.1 Materials

3.1.1 Equipment

- 1.5 mL and 2 mL micro tubes (Sarstedt)
- 10 cm and 15 cm tissue culture dishes (TPP)
- 15 mL and 50 mL centrifuge tubes (BD Biosciences)
- 15 mm round coverslips (Electron Microscopy Sciences)
- 96-well MaxiSorp microtiter plate (Nunc)
- 96-well microtiter black plate (Greiner)
- 96-well microtiter cell culture black plate with transparent bottom (Corning)
- 96-well microtiter cell culture transparent plate (TPP)
- 96-well microtiter transparent plate (Costar)
- Automatic pipettes (Eppendorf)
- Cell line incubator (Binder)
- Centrifuges (Eppendorf)
- Concentrator 5301 (Eppendorf)
- Gel casting kit MiniProtean (Biorad)
- Gel imaging system G:Box (Syngene)
- Homogenizer Ultraturrax (IKA)
- Image software Cell-F (Olympus)
- In vivo imaging system IVIS (Perkin Elmer)
- Inverted microscope Olympus IX81 (Olympus)
- Laminar air flow cabinet for cell culture BSB 4A (Gelaire Flow Laboratories)
- Microplate reader TECAN Infinite M1000 (Tecan)
- Microscope slides (Assistent)
- Mini-Extruder (Avanti Polar Lipids)
- Nanodrop ND-1000 (Babtech International)
- Neubauer chamber (Carl Roth)
- Nitrocellulose membrane
- pH-meter MP 220 (Mettler Toledo)
- Polycarbonate membrane, pore size 100 nm (GE Healthcare)
- Power supply Western Lightning Volt™ Power Supply OSP-300 (Thermo Scientific)
- Ultra centrifugal filters Amicon Ultra-4 and Ultra-15, MWCO 50 kDa (EMC Millipore)
- Vertical Electrophoresis Lab Apparatus MiniProtean Tetracell (Biorad)
- Western transfer apparatus TE22 Mighty Small Transphor Unit (GE Lifesciences)

- Zeta potential analyzer ZetaPALS (Brookhaven Instruments)

3.1.2 Chemicals and commercial kits

- BrdU cell proliferation ELISA (Roche)
- BSA (Sigma-Aldrich)
- Bz-Phe-Val-Arg-AMC (Bachem)
- cholesterol (Sigma)
- DiR' (Thermo Fisher Scientific)
- DMSO (Merck)
- DTT (Sigma-Aldrich)
- E-64 (Bachem)
- EDTA (Serva)
- FBS (Sigma-Aldrich)
- Glutamine (Gibco-Invitrogen)
- Isofluorane (Vetpharma Animal Health)
- L-a-phosphatidylcholine (Avanti Polar Lipids)
- L-Cys (Sigma-Aldrich)
- LysoTracker Green
- Methanol (Merck)
- MTT (Sigma)
- NaCl (Serva)
- PE Lissamine Rhodamine B (Avanti Polar Lipids)
- PE maleimide-PEG (Avanti Polar Lipids)
- PE methoxy-PEG (Avanti Polar Lipids)
- Penicillin/Streptomycin (Gibco-Invitrogen)
- Prestained Protein Ladder PageRuler (MBI Fermentas)
- SDS (Thermo Fisher Scientific)
- TCEP (Thermo Fisher Scientific)
- Total protein concentration assay (Biorad)
- TRIS (Serva)
- Triton X-100
- Trypan Blue (Sigma-Aldrich)
- TrypleSelect trypsin (Gibco, Invitorgen)
- Tween-20 (Sigma-Aldrich)
- Western Blotting Detection Reagents ECL™ (GE Healthcare)
- z-Arg-Arg-AMC (Bachem)
- z-Phe-Arg-AMC (Bachem)

3.1.3 Buffers, solutions, and media

- PBS
  6.6 mM Na_2HPO_4
  13.4 mM NaH_2PO_4
  150 mM NaCl
  pH 7.0

- PBST
  PBS
  0.005% Tween-20

- PBST-BSA
  PBST
  0.5% BSA

- Solution for SDS-PAGE stacking gel
  1.33 mL 40% acrylamide-bisacrylamide
  2.5 mL 0.5 M Tris/HCl (pH 6.8)
  6.4 mL H2O
  0.1 mL 10% SDS
  0.05 mL 10% APS
  0.025 mL TEMED

- Solution for SDS-PAGE resolving gel
  3.75 mL 40 % acrylamide-bisacrylamide
  2.5 mL 1 M Tris-HCl (pH 8.8)
  3.6 mL H2O
  0.1 mL 10% SDS
  0.05 mL 10% APS
  0.005 mL TEMED

- SDS-PAGE loading buffer (6x)
  375 mM Tris-HCl
  6% SDS
  48% glycerol
  100 mM DTT
  0.03 % bromophenol blue
  pH 6.8

- SDS-PAGE buffer
  25 mM Tris
  192 mM L-Gly
  0.1 % SDS

- Western transfer buffer
  25 mM Tris
  192 mM L-Gly
  15 mM SDS
  20% methanol

- Tissue lysate buffer
  250 mM Tris-HCl, pH 7.0
  5 mM EDTA
  1% Triton X-100

- Cathepsin L activity buffer
  89.7 mM sodium acetate
  10.3 mM acetic acid
  5 mM DTT
  pH 5.5

- Cathepsin S activity buffer

35.7 mM Na_2HPO_4
64.3 mM NaH_2PO_4
5 mM DTT
pH 6.5

- Complemented DMEM (cDMEM)
  DMEM (Sigma)
  10 % FBS
  1 % Penicillin/Streptomycin
  2 mM Glutamine

3.1.4 Antibodies

- Rabbit polyclonal anti-6X His tag antibodies (ab9108, Abcam)
- Rabbit polyclonal anti-cathepsin S antibodies (ab232740, Abcam)
- Goat polyclonal anti-cathepsin L antibodies (AF1515, R&D Systems)
- HRP-conjugated goat polyclonal anti-rabbit IgG antibodies (Jackson Immunoresearch)
- HRP-conjugated donkey polyclonal anti-goat IgG antibodies (Abcam)

3.1.5 Recombinant proteins

- Human and mouse cathepsins S and L were expressed in *Pichia pastoris* as described previously (Mihelic, Dobersek, Guncar, & Turk, 2008)
- Stefin A [D61C] was expressed in the soluble fraction in *Escherichia coli*
- Wild type stefin A

3.1.6 Mammalian cell lines

- A549: human lung carcinoma cell line
- B16F10: murine skin melanoma cell line
- HeLa: human cervical adenocarcinoma cell line
- MCF-7: human breast ductal carcinoma cell line
- MDA-MB-231: human breast adenocarcinoma cell line
- L929: immortalized murine fibroblast cell line
- MEF: primary murine embryonic fibroblasts
- HEK293: human embryonic kidney cell line
- PyMT: primary murine tumor cells from PyMT-MMTV mammary gland adenocarcinoma

3.1.7 Mice

- Wild type FVB/N mice
- MMTV-PyMT transgenic FVB/N mice

3.2 Methods

3.2.1 Liposomes

3.2.1.1 Liposome preparation

Six different liposome types were prepared as listed in Table 1.

Table 1: Types of liposomes prepared and their naming.

Dye	No dye	Rhodamine B	DiR'
No ligand	LP	Rho-LP	DiR'-LP
Stefin A [D61C]	stA-LP	stA-Rho-LP	stA-DiR'-LP

Liposomes were prepared by mixing chloroform dissolved lipids as listed in Table 2. The organic solvent was then evaporated in an Eppendorf Concentrator 5301. The dry lipid film formed was then hydrated in degassed PBS. After hydration, the total lipid concentration was 30 mM. In order to generate nanosized unilamellar bilayer liposomes, the multilamellar formed vesicles were extruded by a mini-extruder with a polycarbonate membrane with a pore size 100 nm.

Table 2: Lipid composition of liposomes: molar % of lipid components are listed for each type of liposomes prepared (LP, Rho-LP and DiR'-LP).

Lipid component	LP/stA-LP	Rho-LP/stA-Rho-LP	DiR'-LP/stA-DiR'-LP
L-a-phosphatidylcholine	63	62.9	62.5
cholesterol	32	32	32
PE methoxy-PEG	4	4	4
PE maleimide-PEG	1	1	1
PE Lissamine Rhodamine B	/	0.1	/
DiR'	/	/	0.5

3.2.1.2 Liposome functionalization

In order to functionalize the prepared liposomes, stefin A [D61C] was incubated with 5 mM TCEP for 30 min at room temperature to ensure the Cys61 residue is reduced. The reduced stefin A [D61C] was added to the liposome suspension to the final concentration of 15 μM. After slight shaking at room temperature for 1.5 h, the reaction was terminated by the addition of 10 mM L-cysteine. After conjugation, the residual unconjugated stefin A [D61C] was removed by ultrafiltration in Amicon Ultra-4 centrifugal Filter Units. Non-functionalized liposomes were exposed to the same conditions, however, no stefin A [D61C] was added to the suspension.

Liposomes were then mixed with SDS-PAGE loading buffer, followed by SDS-PAGE and immunoblotting using anti-6X His tag antibodies.

3.2.1.3 Dynamic light scattering (DLS) analysis of liposomes

To determine their size, the prepared liposomes were diluted 1:100 in PBS and analyzed by DLS using ZetaPALS.

3.2.2 Protein analysis

3.2.2.1 Protein concentration determination

The concentration of isolated recombinant proteins was determined by measuring A_{280} with NanoDrop, using the molar extinction coefficient (ε_{280}) to calculate the concentration from the formula $A280 = c \cdot \varepsilon 280 \cdot l$, where l stands for the optical path length.

The total protein concentration in lysates was determined using a modified Bradford assay, where the absorption maximum of Coomassie Brilliant Blue G-250 shifts from 465 nm to 595 nm after binding to aromatic amino acid residues. Bovine serum albumin (BSA) was used as an external standard in the concentration range 1 – 10 µg/mL. Appropriate volumes of BSA stock solution and of diluted samples were pipetted into the wells of a clear 96-well plate and dH2O was added to the final volume of 160 µL. 40 µL of a 5× BioRad Reagent solution was added to the wells and mixed by pipetting. A595 was measured using the Tecan plate reader Infinite M1000. A standard curve was plotted using the measurements of the BSA standard and the concentrations of the samples were calculated from the standard curve.

3.2.2.2 Sodium dodecyl sulfate-polyacrylamide gel electrophoresis (SDS-PAGE)

8 mL of the solution for SDS-PAGE separating gel was poured into the gel casting apparatus. 0.5 mL of isopropanol was added. After 30 min, isopropanol was removed, the stacking gel washed with dH_2O and 2 mL of the solution for SDS-PAGE stacking gel was poured over. A comb with 10 wells was added. After 30 min the comb was removed and the gel was transferred to the tank of the electrophoresis apparatus, which was then filled with SDS buffer. Samples and 6 µL of the prestained protein ladder were loaded into the wells. Electrophoresis ran at a constant current of 0.8 mA · cm2 of gel until the standards were separated.

3.2.2.3 Western transfer and immunoblotting

A piece of nitrocellulose membrane and several pieces of filter paper of the same size as the polyacrylamide gel were soaked in the Western transfer buffer. The unit for Western transfer was assembled as follows: the polyacrylamide gel was placed on five filter papers, the membrane was placed over the gel and five more filter papers were placed over it. Any air bubbles were carefully removed and the unit was placed into the tank for Western transfer, which was filled with the Western transfer buffer. The transfer ran for 2 h at the current 250 mA.

After the transfer, the membrane was incubated in the TBST-BSA solution for 30 min at room temperature, in order to block the non-specific protein binding sites. Then primary antibody solution in TBST-BSA was added to the membrane and incubated overnight at 4 °C. After that, the membrane was washed for 1 h in TBST, which was changed several times. The membrane was then incubated with secondary antibody solution in TBST for 1 h and washed again for 1 h with TBST. For detection, the commercial kit for chemiluminescence Amersham ELC Western Blotting Detection Reagents was used following the manufacturer's instruction. 1 mL of the reagent was placed on the membrane and after 2 min the membrane was imaged in the gel imaging system G:Box (Syngene).

3.2.2.4 Solid-phase affinity assay

Recombinant cathepsins S or L (200 nM) in PBS were immobilized to a 96-well MaxiSorp plate by overnight incubation at 4 °C. The remaining non-specific binding sites were blocked by incubating the plate with 3 % BSA in PBS for 1 h at room temperature. After that, solutions of stA-Rho-LP and Rho-LP in PBS were added to the plate and incubated for 1h at 4 °C. The plate was then washed 3 times with PBS and fluorescence intensity was measured using the Tecan Infinite M1000 plate reader at excitation and emission wavelengths of 560 and 580 nm, respectively.

3.2.3 Enzyme activity

3.2.3.1 Active site titration

Cathepsins S and L were first active-site titrated using the irreversible cysteine protease inhibitor E-64. 10 µM solutions of cathepsin S or cathepsin L in the appropriate activity buffers were incubated with increasing concentrations of E-64 in a black 96-well plate for 30 min at 37 °C. To start the reaction, the appropriate substrate was added (Bz-Phe-Val-Arg-AMC for cathepsin S or z-Phe-Arg-AMC for cathepsin L) to the final concentration of 10 µM. Fluorescence was measured with the Tecan Infinite M1000 plate reader at excitation and emission wavelengths of 340 and 450 nm, respectively. The residual activity was calculated from the slopes of the increasing fluorescence. Residual activity versus inhibitor concentration was plotted and the active concentration of the enzymes was calculated from the graph.

Active concentrations of wild type stefin A and stefin A [D61C] were determined with the same approach, using active site titrated cathepsin L.

3.2.3.2 Effect of liposomes on cathepsins S and L activity

Cathepsin S or cathepsin L were mixed with increasing concentrations of stA-LP or LP in the appropriate activity buffers (cathepsin S activity buffer and cathepsin L activity buffer, respectively) in a black 96-well plate and incubated for 30 min at 37 °C. The substrate was then added and the fluorescence measured, as described for the active site titration above.

3.2.3.3 Determining the inhibition constants (K_i)

Inhibition constants were determined for wild type stefin A or stefin A [D61C] and human or mouse cathepsin S or L. Increasing concentrations (0-12 nM) of wild type stefin A or stefin A [D61C] were mixed with the substrate (60 µM z-Phe-Arg-AMC for cathepsin S or 80 µM z-Arg-Arg-AMC for cathepsin L) incubated in the appropriate activity buffers (cathepsin S activity buffer or cathepsin L activity buffer) for 15 min at 37 °C. To start the reaction, the enzyme was added to the final concentration of 100 pM for human cathepsin L or 500 pM for mouse cathepsin L, human and mouse cathepsin S. Fluorescence was measured as described above. Residual activity versus inhibitor concentration was plotted. K_i was determined according to the Morrison equation for tight inhibition.

3.2.4 Cell culturing methods

3.2.4.1 Growing and passaging cells

Cell lines were grown in an incubator at 37 °C and 5 % CO2. Cells were grown in cDMEM. When cells grew to confluence, they were washed with PBS two times and TrypleSelect

trypsin was added to detach them. After 5 min of incubation at 37 °C, cDMEM was added to stop the trypsinization. The cell suspension was then diluted 1:6 in cDMEM and transferred to a new plate.

3.2.4.2 Cell viability assay

Cell viability was tested with the MTT (3-(4,5-dimethylthiazol-2-yl)-2,5-diphenyltetrazolium bromide) tetrazolium reduction assay. In viable cells, MTT is converted into insoluble purple-colored formazan product and is thus a marker of an active metabolism.

Cells were seeded into clear cell culture 96-well plates, 10000 cells/well. Next day, nanoparticles in cDMEM were added to the wells and incubated for 24 h. After that, cells were washed with PBS and MTT (10 mg/mL in PBS) was added. After 2 h, MTT was removed and DMSO was added to dissolve the formazan crystals. Absorbance was measured at 570 nm with the Tecan Infinite M1000 plate reader.

3.2.4.3 Proliferation assay

Proliferation was analyzed using the BrdU (5-bromo-2'-deoxyuridine) proliferation assay. BrdU is a synthetic analog of thymidine and incorporates into newly synthesized DNA in proliferating cells. It can be detected with specific antibodies.

Cells were seeded into black cell culture 96-well plates with a clear bottom, 5000 cells/well. The next day, nanoparticles in cDMEM were added to the wells and incubated for 24 h. BrdU proliferation assay was then used according to the manufacturer's instructions. In short, cells were fixed, anti-BrdU antibodies were added and after 90 min, cells were washed and the substrate was added. Luminescence was then measured with the Tecan Infinite M1000 plate reader.

3.2.4.4 Analysis of lysosomal integrity

Cells were seeded on cover glasses, which were placed in 12-well plates. When they reached 80 % confluence, cDMEM with 1 mg/mL Aloohene was added and incubated for 6 h. The medium was then replaced and Lysotracker Green (20 nM in cDMEM) was added. After 7 min, cells were washed with PBS and Hoechst33342 (10 µg/mL in PBS) was added. After 10 min, cells were washed again and cover glasses were placed on objective glasses and observed using the inverted microscope Olympus IX81.

3.2.4.5 Conditioned media pH measurement

Cells were seeded in 12-well plates. When they reached 80 % confluence, DMEM with 0-1000 µg/mL Aloohene was added. After 20 h of incubation, conditioned media was collected and pH was measured, using pH-meter MP 220 (Mettler Toledo).

3.2.5 Animal studies

3.2.5.1 Ethical committee approval

Mice were used in accordance with the protocols approved by the Veterinary Administration of the Republic of Slovenia (VARS) and the government Ethical Committee. Procedures for animal care and use were in accordance with the "PHS Policy on Human Care and Use of Laboratory Animals" and the "Guide for the Care and Use of Laboratory Animals" (NIH publication 86-23, 1996).

3.2.5.2 Preparing primary PyMT tumor cells

Primary PyMT tumor cells were isolated from transgenic PyMT mice mammary gland tumors as described earlier (Vasiljeva et al., 2006). Cells were grown in cDMEM.

3.2.5.3 Preparing PyMT orthotopic (OT) model

Primary PyMT tumor cells were grown to subconfluency, detached by trypsinization and resuspended in DMEM at a density of 1×10^7 cells mL^{-1}. One hundred µL of cell suspension was then inoculated into the left mammary gland of the congenic FVB/N female mice. Tumors were allowed to grow for 2-3 weeks.

3.2.5.4 *In vivo* imaging of stA-DiR'-LP with the IVIS Spectrum

PyMT OT model mice were used for the *in vivo* imaging experiment. Mice were distributed in three groups as shown in Table 3. Mice in the E-64 group received a daily intratumoral injection of 0.1 mg/kg E-64 in PBS for 5 days. After 5 days, mice received 100 µL of stA-DiR'-LP or DiR'-LP in PBS (3 mM total lipid concentration) by intravenous administration. 5 min after liposome administration, mice were anesthetized with 3 % isofluorane and transferred to the IVIS Spectrum small animal imaging system, where isofluorane anesthesia (1.5 % isofluorane) was maintained during the imaging. Fluorescence imaging was performed for 30 min using the ex/em = 745/800 bandpass filters and a CCD camera.

Table 3: Groups in the in vivo experiment.

	Control group	stA-LP group	E-64 group
Pre-treatment	/	/	E-64
Imaging agent	DiR'-LP	stA-DiR'-LP	stA-DiR'-LP

3.2.5.5 Tumor lysates

Tumors were harvested after the *in vivo* imaging experiment. Tumor lysates were prepared by tissue disruption. 50 µg of tumor tissue was disrupted in 200 µL of tissue lysis buffer using Ultra-turrax. Tumor extracts were then boiled in SDS-PAGE loading buffer, followed by SDS-PAGE and immunoblotting using rabbit polyclonal anti-cathepsin S antibodies and goat polyclonal anti-cathepsin L antibodies.

Proteolytic activity was also measured in tumor lysates. Tumor lysates were diluted in cathepsin L activity buffer. Substrate (z-Phe-Arg-AMC or Bz-Phe-Val-Arg-AMC) was added to the final concentration of 10 µM. Fluorescence was then measured with the Tecan Infinite M1000 plate reader at excitation and emission wavelengths of 340 and 450 nm, respectively.

3.2.6 Statistical analysis

Quantitative data are presented as means ± standard error. Differences were compared using Student's t-test. When P-values were 0.05 or less, differences were considered statistically significant.

Chapter 4

Results

4.1 Targeting Cathepsin S and L with Stefin A [D61C]-Conjugated Liposomes

4.1.1 Preparation of stefin A [D61C]-functionalized liposomes

4.1.1.1 Inhibition of cathepsins S and L by stefin A [D61C]

To be able to functionalize the surface of liposomes with stefin A, we chose to use the reaction between a maleimide and thiol, which is one of the most commonly used protein labeling reactions (Dimasi et al., 2017; Shen et al., 2012). Since stefin A contains no cysteines, we had to use a mutant form, where Asp61 is replaced with a Cys (stefin A [D61C]). This mutation is located on the inhibitor molecule surface opposite from the interaction site with cathepsins (Figure 5) and therefore not expected to interfere with binding and inhibition of cathepsins.

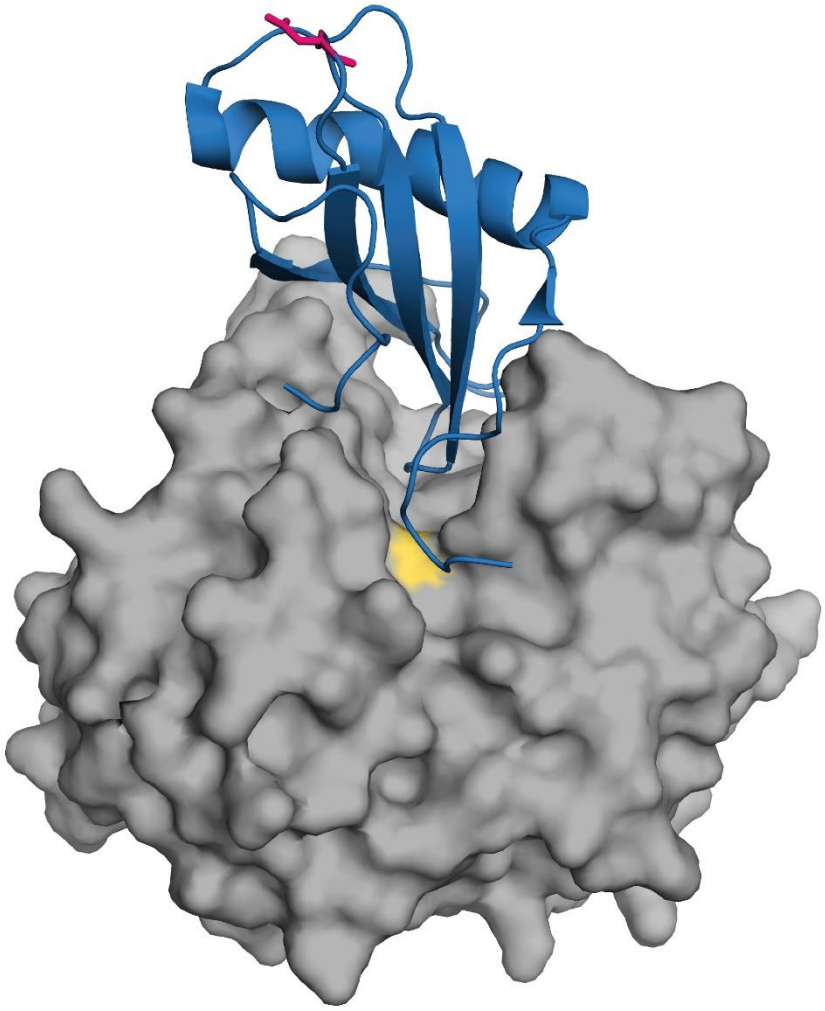

Figure 5: Structure of stefin A-cathepsin B complex (PDB ID: 3K9M). Stefin A Asp61 is colored blue and cathepsin B active site Cys is colored yellow. The image was produced in PyMOL (www.pymol.org).

To test whether stefin A [D61C] retains cathepsin inhibiting properties, we determined the inhibition constants (K_i) for inhibition of human and mouse cathepsins S and L by wild type stefin A and stefin A [D61C] (Table 4). The determined K_i values were in sub-nanomolar range and the values for the mutant inhibitor were comparable to the wild type inhibitor.

Table 4: Inhibition constants (K_i) for inhibition of cathepsins L and S by stefin A and stefin A [D61C] mutant.

	K_i (nM)	
Enzyme	Stefin A	Stefin A [D61C]
Human cathepsin L	0.014 ± 0.002	0.0034 ± 0.0008
Mouse cathepsin L	0.02 ± 0.01	0.016 ± 0.008

Human cathepsin S	0.083 ± 0.009	0.061 ± 0.007
Mouse cathepsin S	0.27 ± 0.08	0.21 ± 0.04

4.1.1.2 Conjugation of stefin A [D61C] to liposomes

Liposomes were prepared by extrusion through a polycarbonate membrane and contained PE maleimide-PEG, which is a lipidated PEG, functionalized with a maleimide group (Figure 6). Stefin A [D61C] was then conjugated to the liposome surface through the maleimide-cysteine reaction, resulting in the formation of a covalent non-reducible thio-ester bond. Liposomes were also functionalized with a fluorescent dye to enable detection.

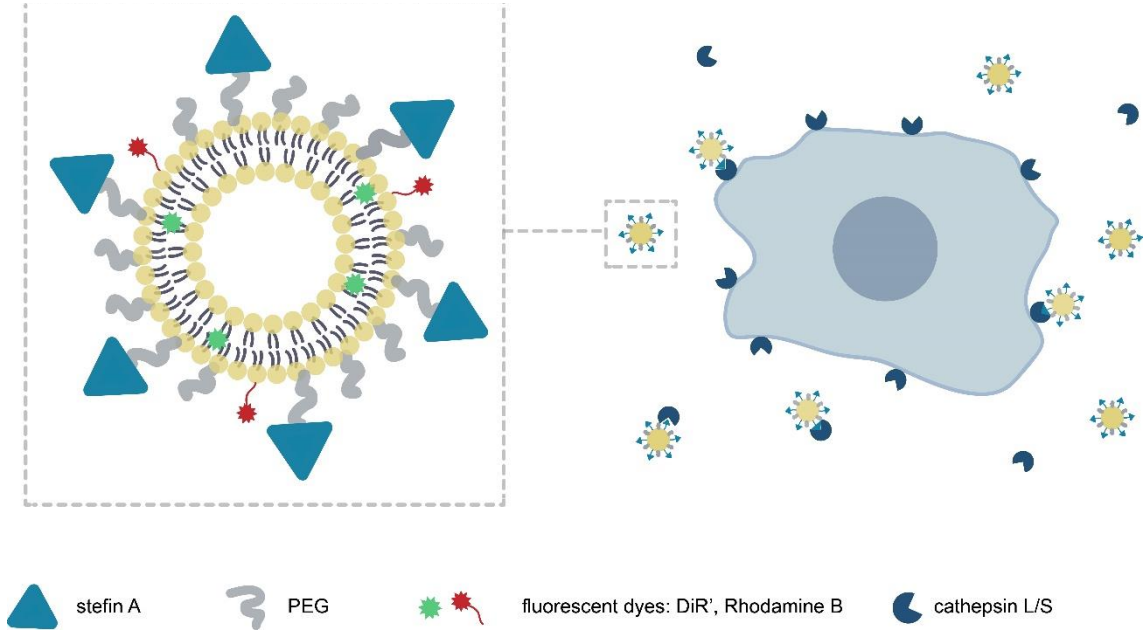

Figure 6: Liposomal targeting system approach. Liposome surface is functionalized with stefin A as the targeting ligand for binding to cathepsins L and S. Fluorescent dye can be used for detection. PEG is introduced to create stealth liposomes, which have a longer circulation time *in vivo*. The functionalized liposomes bind to cell membrane-associated cathepsins or cathepsins secreted to the microenvironment.

The efficiency of the conjugation of stefin A [D61C] was verified by Western blotting (Figure 7). Most of the protein was successfully conjugated to the lipid, as shown by the shift of the stefin A [D61C] band (15 kDa) to a higher molecular weight. Based on the literature, the expected efficiency was approximately 70 % (Martinez-Jothar et al., 2018), however, the very slight band corresponding to the unconjugated protein indicates that the efficiency could be higher. The remaining unconjugated protein was removed by ultrafiltration.

Figure 7: Stefin A [D61C] conjugation to liposomes was confirmed by western blotting: stA – stefin A [D61C], stA-LP – stefin A [D61C]-conjugated liposomes, stA-LP* – stefin A [D61C]-conjugated liposomes after the removal of unconjugated stefin A [D61C] with ultrafiltration, LP – control liposomes.

The size distribution of the prepared liposomes was analyzed with DLS (Figure 8). The average diameter of stefin A [D61C]-conjugated liposomes was 179.5 nm.

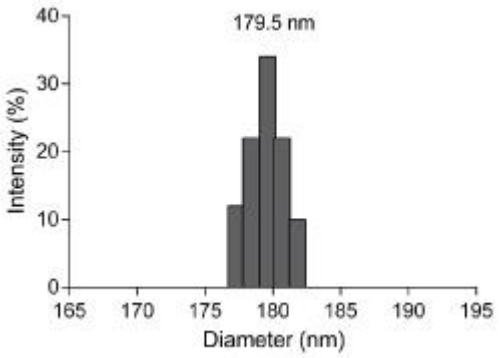

Figure 8: DLS measurement of stefin A [D61C]-conjugated liposomes, showing the distribution of diameters and the average size.

4.1.2 Stefin A [D61C]-conjugated liposomes *in vitro* binding and inhibition of recombinant cathepsins L and S

4.1.2.1 *In vitro* binding of liposomes to cathepsins L and S

To confirm that the stefin A [D61C] conjugated to the liposome surface still retained the ability to bind to cathepsins L and S, a solid phase affinity assay was performed. Liposomes were labeled with rhodamine B, a fluorescent dye, to enable their detection. Stefin A [D61C]-liposomes (StA-Rho-LP) or non-functionalized liposomes (Rho-LP) were incubated with recombinant cathepsin S or L, immobilized on a plate. The binding was confirmed by an increase in fluorescence. As shown in Figure 9, the fluorescent signal for StA-Rho-LP was higher than for Rho-LP, thus confirming the binding of liposomes to recombinant cathepsins S and L.

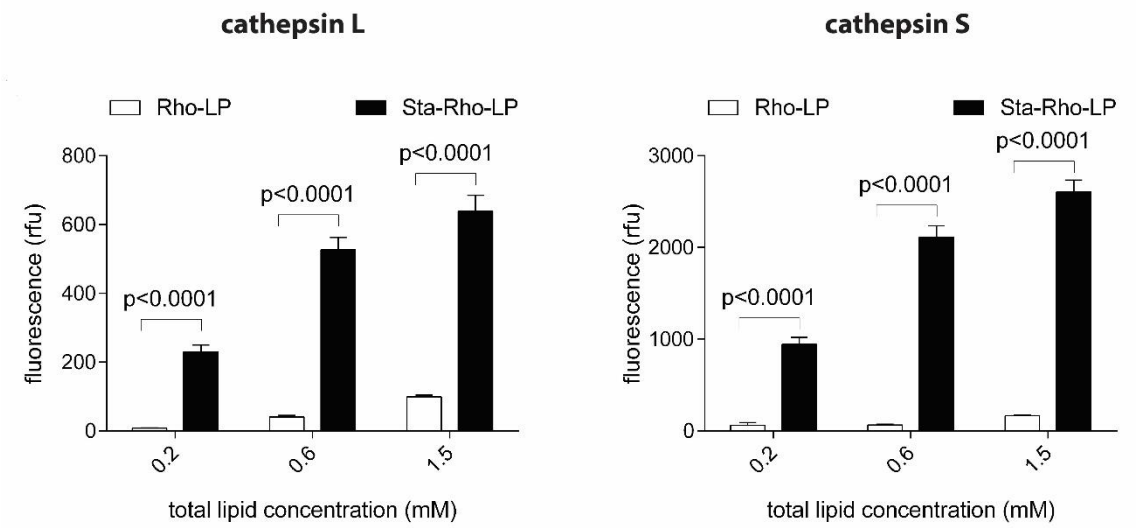

Figure 9: Solid-phase affinity assay with immobilized recombinant cathepsin (200 nM). Increasing concentrations of non-functionalized rhodamine-labeled liposomes (Rho-LP) or stefin A [D61C]-conjugated rhodamine-labeled liposomes (stA-Rho-LP) were incubated in 96-well plates with immobilized recombinant cathepsin L or recombinant cathepsin S. After washing, binding was detected by fluorescence measurement (ex/em = 560/580 nm).

4.1.2.2 *In vitro* inhibition of liposomes to cathepsins L and S

Liposomes were also tested for their ability to inhibit recombinant cathepsin S and L. The addition of increasing concentrations of stA-LP resulted in a linear decrease in cathepsin S or L activity, while the addition of LP had no effect on the activity (Figure 10).

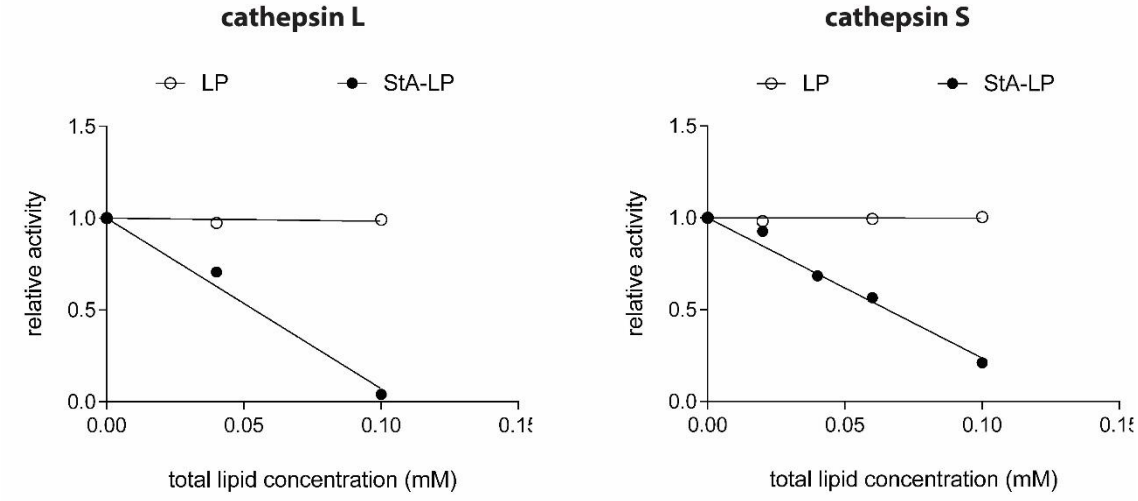

Figure 10: Inhibition of recombinant cathepsin L and recombinant cathepsin S activity. Relative activity (ratio of inhibited vs. uninhibited enzyme activity) was determined in the presence of increasing concentrations of non-functionalized (LP) or stefin A [D61C]-conjugated liposomes (stA-LP).

This confirmed that stA-LP not only bound but also inhibited recombinant cathepsins S and L, thus the inhibitory activity was conserved after conjugation. The inhibition could also provide an additional therapeutic benefit.

4.1.3 *In vivo* imaging of stefin A [D61C]-functionalized liposomes

The efficiency of the developed liposomal system for targeting cathepsins S and L was then evaluated *in vivo*, using a mammary cancer model based on orthotopic transplantation of primary tumor cells isolated from mammary tumors developed in mice carrying polyoma virus middle T oncogene (PyMT) (Mikhaylov et al., 2011). Elevated levels of cysteine cathepsins were reported for this transgenic mouse model, therefore making it appropriate for testing our stA-LP delivery system.

When the tumors reached an average size of 200 mm^3, mice were dosed with stA-LP containing a lipophilic fluorescent dye DiR' and imaged for 30 min. To demonstrate the selectivity of the stA-LP for cathepsins, one group of mice received the cysteine cathepsins inhibitor E-64 intratumorally for five days before the day of the experiment and was then dosed with stA-DiR'-LP (Figure 11).

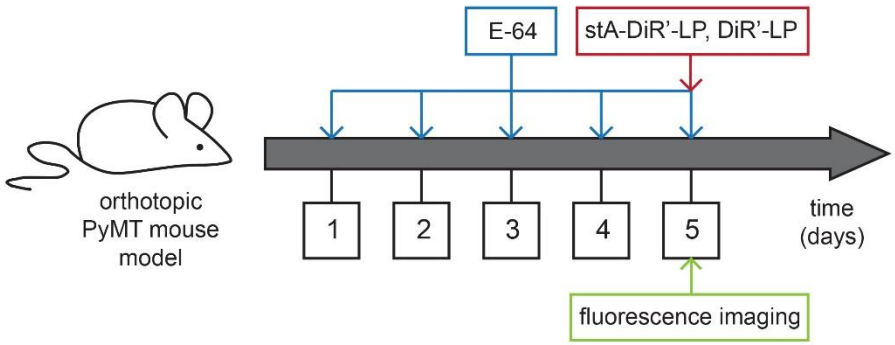

Figure 11: Time scheme of the *in vivo* experiment. Mice were dosed with control (DiR'-LP) or stefin A-conjugated liposomes (stA-DiR'-LP) by intravenous injection. In the E-64 group, mice were pre-treated with E-64 by intratumoral injection.

The fluorescent signal at the tumor site was significantly elevated in mice that received stA-DiR'-LP, compared to the control group that received non-conjugated DiR'-LP (Figure 12). Pre-treatment of mice with E-64 reduced the fluorescent signal significantly, therefore corroborating the specificity of the system. A low accumulation of the fluorescent signal was also present in the group that received DiR'-LP; this can be attributed to the enhanced permeability and retention (EPR) effect (Nakamura, Mochida, Choyke, & Kobayashi, 2016; Ngoune et al., 2016).

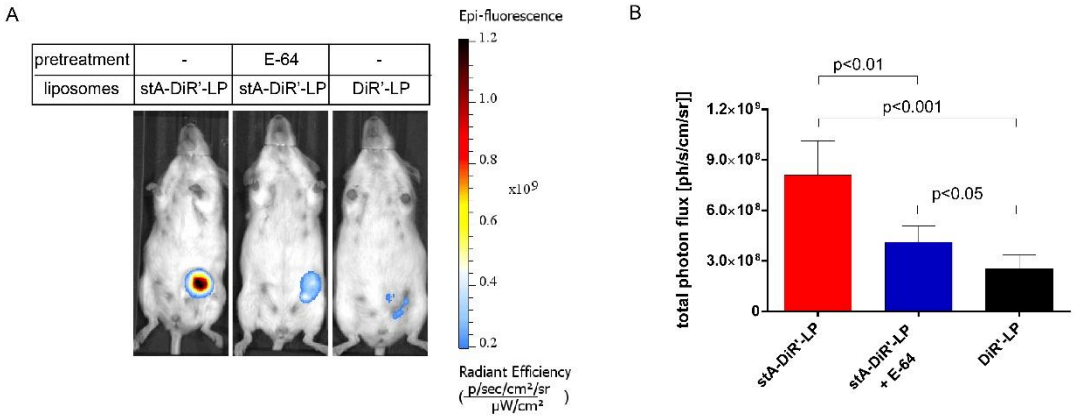

Figure 12: *In vivo* imaging of mice bearing PyMT cells based mammary tumors. (A) Representative images of mice from each group. (B) Total photon flux from the tumor region was calculated.

In the next step, we evaluated the effect of the E-64 pre-treatment on the expression levels and processing of cathepsins S and L in tumors by immunoblotting the tumor lysates. As shown in Figure 13, there were no differences in expression or activation of cathepsin S and L between the on-treated tumors, tumors pre-treated with E-64 and tumors dosed with stA-LP.

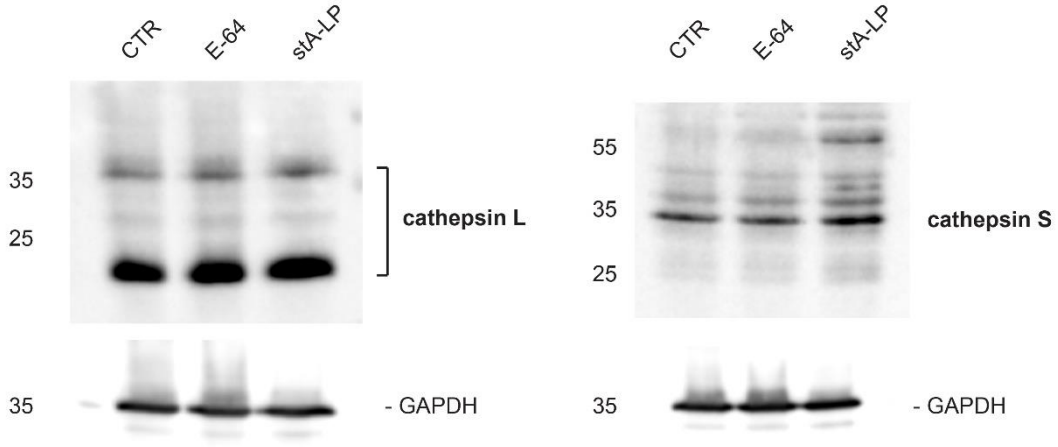

Figure 13: Western blots of tumor lysates showing the presence of cathepsin S and cathepsin L in mice with no pre-treatment, mice with E-64 pre-treatment and mice injected with stA-LP.

We also measured cathepsins' proteolytic activity in tumor lysates with two different substrates, as shown in Figure 14. Pre-treatment with the inhibitor E-64 successfully blocked cathepsins' proteolytic activity. However, treatment with stA-LP did not affect the activity significantly. The likely reason for this is the fact that stA-LP binds primarily to the extracellular pool of cathepsins, while the majority of cathepsins are localized in the lysosomes. In addition, the concentration of stA-LPs used in the experiments was much lower than that of E-64.

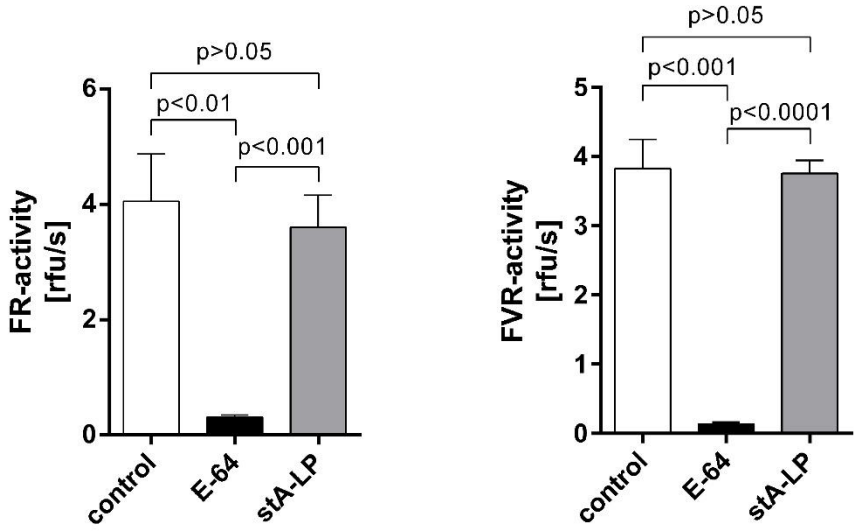

Figure 14: Proteolytic activity in tumor homogenates of mice with no pre-treatment, mice with E-64 pre-treatment and mice injected with stA-LP, measured with Bz-FVR-AMC (FVR-activity) for cathepsin S and with z-FR-AMC (FR-activity) for cathepsin L.

4.2 Effect of Aluminum-Based Nanoparticles on Cells and Their Microenvironment

4.2.1 Effect of aluminum-based nanoparticles on cell viability

In our study, we used nanoparticles represented by agglomerates of radially assembled crumpled AlOOH nanosheets that have been termed Aloohene, referring to its chemical formula AlOOH. In the previous work, it was shown that Aloohene can inhibit tumor growth via dysregulation of ion imbalance in the tumor microenvironment (Lerner et al., 2018). To study how different forms of aluminum-based nanoparticles affected cell viability, we treated different cancerous cell lines (A549, B16F10 and HeLa) with Aloohene and two phases of aluminum nanoparticles, θ- and γ-Al_2O_3. Two concentrations of nanoparticles, 1 and 10 mg/mL were used. As shown in Figure 15A, the lower concentration had minimal effect on cell viability and there were no obvious differences in the effect of the three nanoparticles. Notably, the higher concentration, 10 mg/mL (Figure 15B), had a more marked effect on all the cell lines, as their viability was reduced under 50 % of the untreated control. There was no obvious difference in the effect of Aloohene, θ- or γ-Al_2O_3.

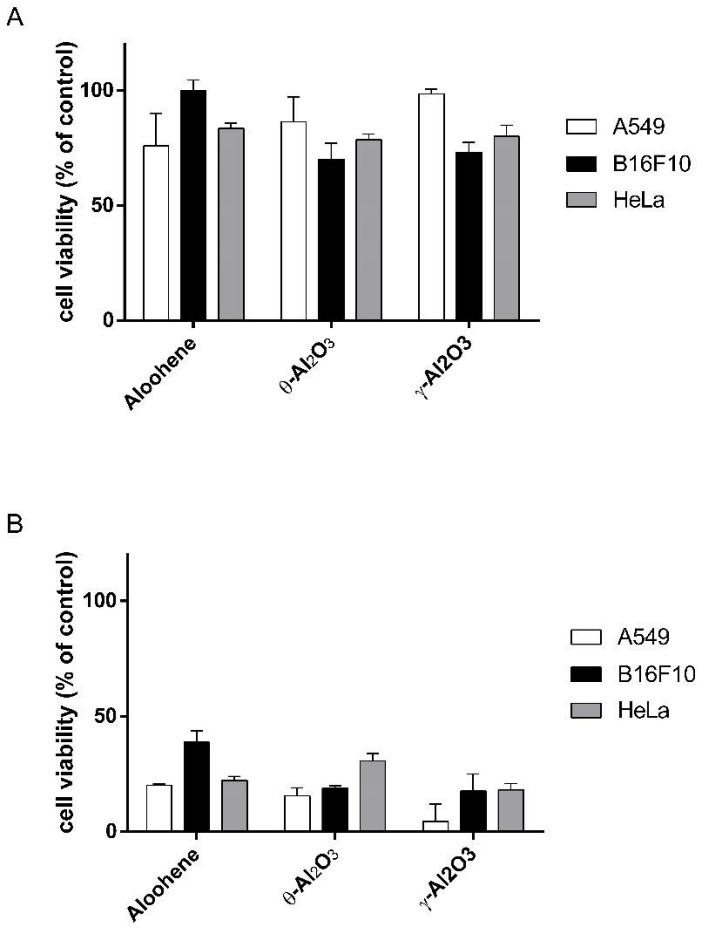

Figure 15: Cell viability after treatment with 1 mg/ml (A) or 10 mg/mL (B) Aloohene, θ - or γ-Al_2O_3. Cell viability of three different cell lines (HeLa, A549 and B16F10) was determined by the MTT assay and is shown as a percentage of untreated control viability.

4.2.2 Effect of aluminum-based nanoparticles on cell proliferation

To analyze the effect of the nanoparticles on cell proliferation three different cancer cell lines were treated with Aloohene and the two selected phases of aluminum nanoparticles, θ- and γ-Al_2O_3. Two concentrations of nanoparticles were used, 1 and 10 mg/mL. As shown in Figure 16A, the lower concentration had almost no effect on cell proliferation in any of the cell lines. However, treatment with higher concentrations had a pronounced effect (Figure 16B). HeLa cells seemed to be the most resistant to the inhibition of proliferation, while B16F10 and A549 cells were more susceptible. Out of the tested nanoparticles, γ-Al_2O_3 had the most effect on cell proliferation.

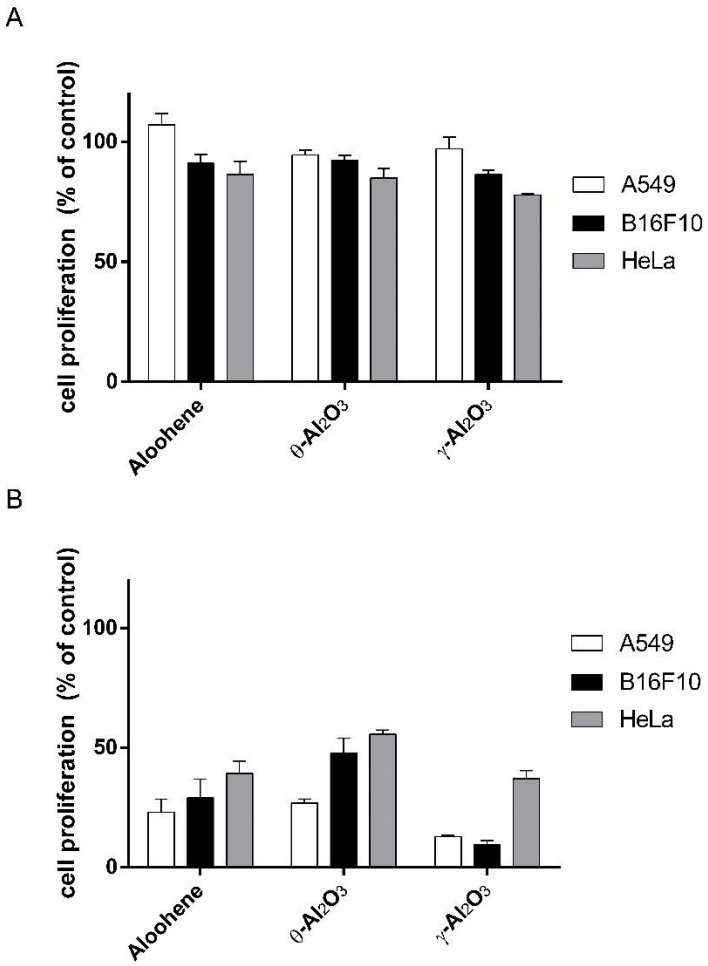

Figure 16: Cell proliferation after treatment with 1 mg/ml (A) or 10 mg/mL (B) Aloohene, θ- or γ-Al_2O_3. Cell proliferation of three different cell lines (HeLa, A549 and B16F10) was determined by the BrdU assay and is shown as a percentage of untreated control proliferation.

4.2.3 Lysosomal integrity following Aloohene treatment

The control of cell proliferation involves diverse signaling pathways, growth factors, and receptors. To determine whether cytotoxicity of Aloohene is caused by lysosomal damage, PyMT cells were treated with Aloohene and lysosomal integrity was analyzed with the LysoTracker Green dye. LysoTracker Green stains acidic compartments, thus labeling lysosomes. Neither shape nor multitude of stained compartments was changed after Aloohene treatment (Figure 17), indicating Aloohene does not damage lysosomes.

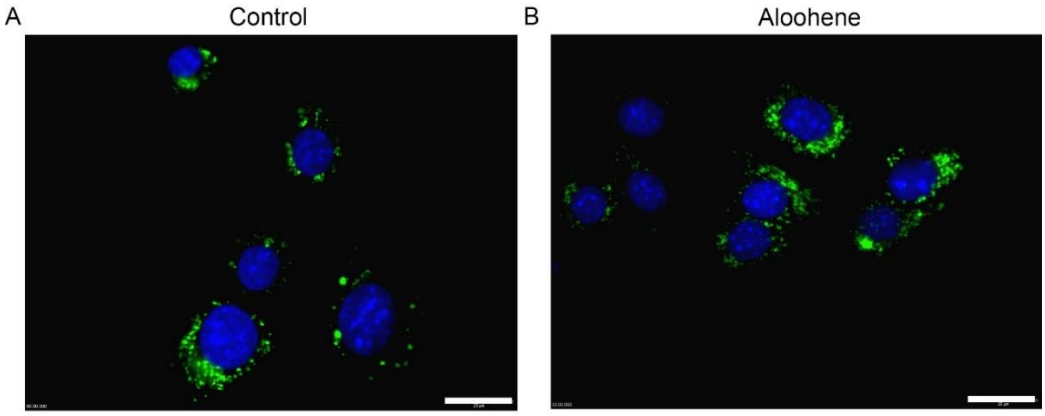

Figure 17: Analysis of lysosomal integrity in MMTV-PyMT cells treated with Aloohene. MMTV-PyMT tumor cells were cultured in the absence (A) and presence (B) of Aloohene for 6 h, then labeled with LysoTracker Green (20 nM) and Hoechst 33342 (10 μg/mL). Cells were imaged using a fluorescence microscope. The scale bar corresponds to 20 μm.

4.2.4 Extracellular pH following Aloohene treatment

The involvement of ion channels in cell proliferation is supported by a wealth of experimental evidence. As such, the dysregulation of cellular Ca^{2+} and pH homeostasis are central steps in the induction of many (apoptotic and other) death pathways. As such, it was proposed that inhibition of acid/base transport could be exploited to sensitize cancer cells to chemotherapy. Therefore, in the following step, the effect of Aloohene on the extracellular pH of PyMT cells was tested. pH was measured in conditioned media (DMEM) after Aloohene treatment. As shown in Figure 18, there was no significant change in conditioned media pH caused by incubation with Aloohene, demonstrating that the mechanism of Aloohene cytotoxicity was not through pH alteration. Taken together, these data indicate that inhibition of tumor cell proliferation does not involve damage of the pH.

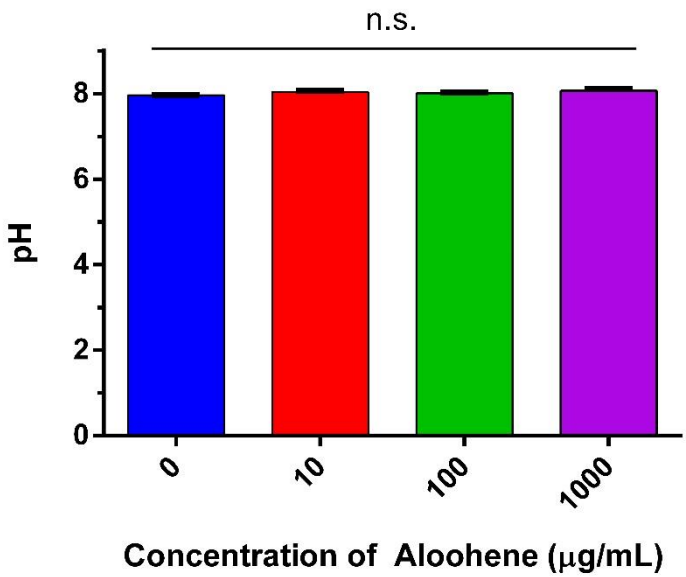

Figure 18: Analysis of MMTV-PyMT cells conditioned medium pH in the presence of Aloohene. MMTV-PyMT tumor cells were cultured in the serum-free medium containing various concentrations of Aloohene (10-1000 μg/mL) during 20 h.

Chapter 5

Discussion

In this thesis, we have developed new tools to target the tumor microenvironment for diagnostic and/or therapeutic purposes. The tumor microenvironment is a complex mixture of various cells and molecules, offering a myriad of targets to exploit in designing new strategies for treating cancer. To achieve this goal, nanoparticles can be used either as a delivery system or as a cytotoxic agent.

Proteases have been considered as therapeutic targets in cancer for a long time, due to their elevated activity in various stages of cancer progression (Abbenante & Fairlie, 2005; Olson & Joyce, 2015; B. Turk, 2006). In contrast to other proteases, such as the MMPs, cathepsins are secreted into the extracellular space mainly in pathological conditions, including cancer. Thus, targeting cathepsins represents a promising and safe strategy, diminishing the risk of affecting healthy tissue (Kramer, Turk, et al., 2017). In the first part of the thesis, we describe the development of a new targeting system – liposomes, functionalized with endogenous protease inhibitor stefin A as a targeting moiety for cysteine cathepsins S and L (Bratovs, Kramer, Mikhaylov, Vasiljeva, & Turk, 2019).

Selecting stefin A, a small endogenous inhibitor, as a targeting agent of a drug delivery system has several advantages. First, stefin A has a high affinity to cathepsins, substantially surpassing that of antibodies. Second, the inhibitor is highly specific for its endogenous targets. Additionally, stefin A is highly thermostable and, due to the absence of disulfide bonds, not sensitive to the reducing environment. Although stefin A was reported previously to be cleaved by another tumor protease, cathepsin D, *in vitro*, the experiments were performed at pH 3.5, which is not physiological (Lenarcic et al., 1988). In this work, we thus selected stefin A as a targeting moiety and have shown that stefin A [D61C] displayed on the surface of nanosized liposomes, can successfully target cysteine cathepsins exposed to the tumor microenvironment during cancer progression. Liposome-conjugated small molecule inhibitor of cathepsin B has been shown previously to successfully target the tumor microenvironment (Mikhaylov et al., 2014). In addition, another approach of targeting this protease was exploited by the use of cathepsin B-specific designed ankyrin repeat protein (DARPin), a genetically engineered antibody mimetic protein (Kramer, Renko, et al., 2017). Employing stefin A as a targeting moiety, we are aiming at binding to at least two proteases of the cysteine cathepsin family, cathepsins S and L. Both of these proteases have a tumor-promoting function and have been shown to be overexpressed and secreted in cancer, thus the concept of targeting both proteases could increase the targeting efficiency of the system. Cathepsin S and L were both reported to be associated with multiple stages of tumor progression (Joyce et al., 2004). Cathepsin S was shown to promote angiogenesis and tumor growth through modulation of angiogenic factors (Burden et al., 2009; B. Wang et al., 2006), whereas cathepsin L was reported to

play an important role in neovascularization (Urbich et al., 2005) as well as in increasing invasiveness and migration (Rousselet et al., 2004; Yang & Cox, 2007). Both cathepsin S and L were demonstrated to cleave E-cadherin (Gocheva et al., 2006) and other cell adhesion molecules (Sevenich et al., 2014; Sobotic et al., 2015). Furthermore, inhibition of cysteine cathepsins has been demonstrated to enhance the effect of chemotherapeutic agents in cell line experiments (Shree et al., 2011) as well as in murine cancer models (Bell-McGuinn, Garfall, Bogyo, Hanahan, & Joyce, 2007; Burden et al., 2012). Although we have not demonstrated inhibition of cathepsins S and L *in vivo*, inhibiting the activity of cysteine cathepsins could contribute to the anti-tumor efficacy of the system.

The selection of liposomes as a delivery system has several advantages, including their low toxicity and high biocompatibility. Especially valuable is the feasibility to functionalize them by either conjugating agents to their surface or loading them with hydrophilic or hydrophobic molecules. Thus, equipped with magnetic resonance contrast agents, radioactive tracers or with ultrasound microbubble contrast agents, stefin A [D61C]-conjugated liposomes might be useful as a diagnostic tool. Furthermore, chemotherapeutic agents could be encapsulated to utilize the liposomes for targeted drug delivery to the tumor. Chemotherapeutics like doxorubicin have already been encapsulated in liposomes and have taken advantage of the EPR effect to achieve passive targeting to the tumor tissue (Barenholz, 2012). However, active targeting of liposomes increases accumulation in the target tissue, as was also confirmed in our study (Figure 12). In active targeting strategies, the targets of the drug delivery system are often receptors on the cell surface, such as folate receptors (R. J. Lee & Low, 1995), transferrin receptors (Zhai et al., 2010), EGFR (Kim & Huang, 2012) or HER-2 (Shmeeda et al., 2009). While these receptors are overexpressed in cancer cells, they are also present in normal tissue, which can lead to on-target side effects. Targeting cathepsins S and L or cathepsin B (Mikhaylov et al., 2014) could thus represent a safer option since these enzymes have been detected extracellularly mainly in pathological conditions. Additionally, cancer cells are not the only cells overexpressing cathepsins in the tumor microenvironment, therefore, targeting cathepsins also targets other cell types, such as TAMs, which can increase the efficiency of treatment and broaden the range of cancer types responsive to the treatment.

Most used moieties for targeted drug delivery are small molecules or peptides, and antibodies (Deshpande et al., 2013). By using a small protein inhibitor, we improved the specificity and affinity compared to small molecules, while having a smaller size compared to antibodies, thereby enabling better penetration to the tumor microenvironment. Furthermore, the relatively large protease-binding region of stefin A encompassing the N-terminal segment and two hairpin loops (Jenko et al., 2003; Renko et al., 2010), combined with high thermostability and a lack of disulfide bonds, support its selection as a potent targeting moiety for targeted drug delivery approaches. Notably, stefin A was already used as a scaffold for peptide presentation (Hoffmann et al., 2010; Stadler et al., 2011; Woodman, Yeh, Laurenson, & Ko Ferrigno, 2005), thus additionally supporting the idea of its application to the *in vivo* targeting approaches.

The second part of this thesis is focused on aluminum-based nanoparticles and their effect on cancer cells and the tumor microenvironment. One of the emerging areas for cancer treatment is based on the sensitivity of cancer cells to deviations from the equilibrium of extra- and intracellular ion concentration (Brisson et al., 2011; Yildirim et al., 2012). Thus, inorganic nanostructured materials with pronounced sorption properties and surface charge, which could modulate ion concentrations across a cell membrane, could be used as anticancer agents.

Aluminum hydroxide is a well-studied antacid (Gitelman, 1988) and selective adsorbent for many chemicals (Cai, Yu, & Jaroniec, 2010; Tanada et al., 2003). For our studies, a boehmite form of aluminum hydroxide was synthesized in the form of crumpled and radially

assembled nanosheets and termed Aloohene (AlOOH). Aloohene has been tested for anti-cancer activity on cell lines as well as *in vivo;* it has triggered cell death and lowered proliferation of human and murine cell lines and has also inhibited tumor growth in murine cancer models (Lerner et al., 2018).

Direct molecular dynamics simulation of the interaction between Aloohene and cell membrane in the medium, modeled to be similar to the biological extracellular environment, has shown that Aloohene causes a redistribution of ionic species in the extracellular fluid (Figure 19). An anionic cloud forms around the Aloohene surface, causing the concentration of anions to drop in the spaces distant from the nanoparticle and increase near its surface. Since it has been reported that a reduction of extracellular Cl^- concentration can inhibit cell growth (Collier & Snyder, 2009; Hiraoka et al., 2010), this could explain the anti-proliferative activity of Aloohene. By regulating the activity of ion channels and transporters, Aloohene could influence ion transport, tumor cell nutrition and vital cellular functions (Lerner et al., 2018).

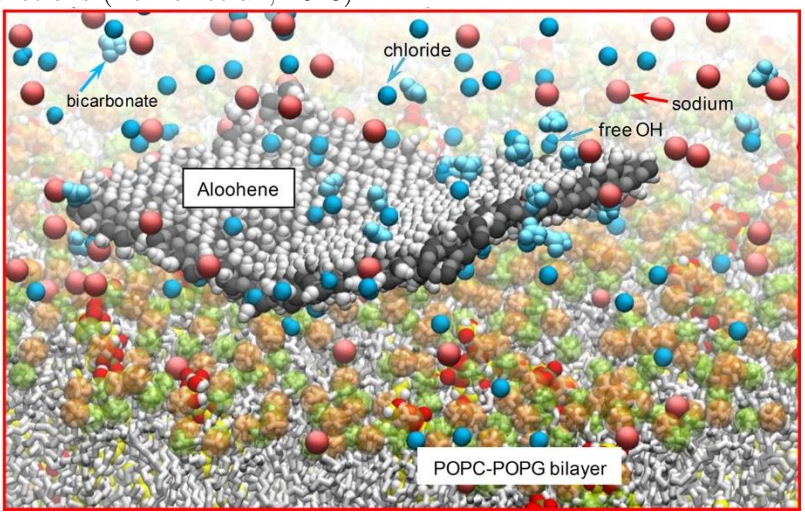

Figure 19: A molecular dynamics simulation of ion redistribution near the cell membrane induced by Aloohene nanosheet. Membrane colors: POPC lipid tails = white, POPC phosphate groups = orange, choline groups = green, POPG lipids = yellow, POPG phosphate groups = red. Aloohene colors: OH groups = white, bridging oxygen = light gray, aluminum = dark gray. Water molecules and lipid hydrogen atoms are not shown. (Lerner et al., 2018)

It has been shown that cancer cells benefit from the lowered pH in the TME and increasing the pH has been demonstrated to inhibit tumor growth (Bellone et al., 2013; Stubbs, McSheehy, Griffiths, & Bashford, 2000). Although some nanoparticles have been designed to modulate local pH (Som et al., 2016), we have demonstrated that Aloohene does not affect extracellular pH in the cell line setting (Figure 18). In addition, lysosomal damage has been proposed as a major mechanism of toxicity of nanoparticles since most of the endocytosed nanoparticles accumulate within lysosomes (Miyayama & Matsuoka, 2016; Panzarini, Inguscio, Tenuzzo, Carata, & Dini, 2013; F. Wang, Salvati, & Boya, 2018). On the contrary, there were no signs of lysosomal damage following treatment with Aloohene (Figure 17), which supports its predominantly extracellular function.

θ- and γ-Al_2O_3 are transition forms of aluminum oxide prepared by heating aluminum boehmite. Their effect on cancer cell line viability and proliferation was shown to be comparable to Aloohene, indicating that new forms of aluminum oxide nanoparticles with anti-cancer activity and potential unique properties could be generated and further investigated for their applicability to new approaches of cancer treatment.

Chapter 6

Conclusions

We developed a new liposome-based targeting system, employing an endogenous small protein inhibitor stefin A to target cysteine cathepsins S and L, representing a new approach in targeted drug delivery. We demonstrated that stefin A-conjugated liposomes accumulate in tumors *in vivo*, and could potentially be useful for cancer diagnostics and treatment.

We determined that Aloohene, an aluminum oxyhydroxide nanoparticle, does not owe its anti-tumor activity to either modulating the extracellular pH or damaging the lysosomes of cancer cells. Aloohene could, however, cause significant ion imbalance in the cell perimembranous space through the selective adsorption of extracellular anions. Aloohene, θ- and γ-Al_2O_3 were shown to have a comparable effect on cancer cell line viability and proliferation, therefore new types of nanoparticles with anti-tumor activity could be generated using these forms of aluminum oxide.

References

Abbenante, G., & Fairlie, D. P. (2005). Protease inhibitors in the clinic. *Med Chem, 1*(1), 71-104.

Adenis, A., Huet, G., Zerimech, F., Hecquet, B., Balduyck, M., & Peyrat, J. P. (1995). Cathepsin B, L, and D activities in colorectal carcinomas: relationship with clinico-pathological parameters. *Cancer Lett, 96*(2), 267-275. doi: 10.1016/0304-3835(95)03930-u

Allen, T. M., & Cullis, P. R. (2013). Liposomal drug delivery systems: from concept to clinical applications. *Adv Drug Deliv Rev, 65*(1), 36-48. doi: 10.1016/j.addr.2012.09.037

Allen, T. M., Hansen, C., Martin, F., Redemann, C., & Yau-Young, A. (1991). Liposomes containing synthetic lipid derivatives of poly(ethylene glycol) show prolonged circulation half-lives in vivo. *Biochim Biophys Acta, 1066*(1), 29-36. doi: 10.1016/0005-2736(91)90246-5

Alphonse, P., & Courty, M. (2005). Structure and thermal behavior of nanocrystalline boehmite. *Thermochimica Acta, 425*(1-2), 75-89.

Balkwill, F. R., Capasso, M., & Hagemann, T. (2012). The tumor microenvironment at a glance. *J Cell Sci, 125*(Pt 23), 5591-5596. doi: 10.1242/jcs.116392

Banerjee, J., Hanson, A. J., Gadam, B., Elegbede, A. I., Tobwala, S., Ganguly, B., . . . Mallik, S. (2009). Release of liposomal contents by cell-secreted matrix metalloproteinase-9. *Bioconjug Chem, 20*(7), 1332-1339. doi: 10.1021/bc9000646

Barenholz, Y. (2012). Doxil (R) - The first FDA-approved nano-drug: Lessons learned. *J Control Release, 160*(2), 117-134. doi: 10.1016/j.jconrel.2012.03.020

Bayda, S., Hadla, M., Palazzolo, S., Riello, P., Corona, G., Toffoli, G., & Rizzolio, F. (2018). Inorganic Nanoparticles for Cancer Therapy: A Transition from Lab to Clinic. *Curr Med Chem, 25*(34), 4269-4303. doi: 10.2174/0929867325666171229141156

Beers, C., Burich, A., Kleijmeer, M. J., Griffith, J. M., Wong, P., & Rudensky, A. Y. (2005). Cathepsin S controls MHC class II-mediated antigen presentation by epithelial cells in vivo. *J Immunol, 174*(3), 1205-1212. doi: 10.4049/jimmunol.174.3.1205

Bell-McGuinn, K. M., Garfall, A. L., Bogyo, M., Hanahan, D., & Joyce, J. A. (2007). Inhibition of cysteine cathepsin protease activity enhances chemotherapy regimens by decreasing tumor growth and invasiveness in a mouse model of multistage cancer. *Cancer Res, 67*(15), 7378-7385. doi: 10.1158/0008-5472.CAN-07-0602

Bellone, M., Calcinotto, A., Filipazzi, P., De Milito, A., Fais, S., & Rivoltini, L. (2013). The acidity of the tumor microenvironment is a mechanism of immune escape that can be overcome by proton pump inhibitors. *Oncoimmunology, 2*(1), e22058. doi: 10.4161/onci.22058

Benavides, F., Perez, C., Blando, J., Contreras, O., Shen, J., Coussens, L. M., . . . Conti, C. J. (2012). Protective role of cathepsin L in mouse skin carcinogenesis. *Mol Carcinog, 51*(4), 352-361. doi: 10.1002/mc.20792

Bratovs, A., Kramer, L., Mikhaylov, G., Vasiljeva, O., & Turk, B. (2019). Stefin A-functionalized liposomes as a system for cathepsins S and L-targeted drug delivery. *Biochimie, 166*, 94-102. doi: 10.1016/j.biochi.2019.05.018

Brisson, L., Gillet, L., Calaghan, S., Besson, P., Le Guennec, J. Y., Roger, S., & Gore, J. (2011). Na(V)1.5 enhances breast cancer cell invasiveness by increasing NHE1-dependent H(+) efflux in caveolae. *Oncogene, 30*(17), 2070-2076. doi: 10.1038/onc.2010.574

Burden, R. E., Gormley, J. A., Jaquin, T. J., Small, D. M., Quinn, D. J., Hegarty, S. M., . . . Scott, C. J. (2009). Antibody-mediated inhibition of cathepsin S blocks colorectal tumor invasion and angiogenesis. *Clin Cancer Res, 15*(19), 6042-6051. doi: 10.1158/1078-0432.CCR-09-1262

Burden, R. E., Gormley, J. A., Kuehn, D., Ward, C., Kwok, H. F., Gazdoiu, M., . . . Olwill, S. A. (2012). Inhibition of Cathepsin S by Fsn0503 enhances the efficacy of chemotherapy in colorectal carcinomas. *Biochimie, 94*(2), 487-493. doi: 10.1016/j.biochi.2011.08.017

Byrne, J. D., Betancourt, T., & Brannon-Peppas, L. (2008). Active targeting schemes for nanoparticle systems in cancer therapeutics. *Adv Drug Deliv Rev, 60*(15), 1615-1626. doi: 10.1016/j.addr.2008.08.005

Cai, W., Yu, J., & Jaroniec, M. (2010). Template-free synthesis of hierarchical spindle-like γ-Al 2 O 3 materials and their adsorption affinity towards organic and inorganic pollutants in water. *Journal of Materials Chemistry, 20*(22), 4587-4594.

Collier, D. M., & Snyder, P. M. (2009). Extracellular chloride regulates the epithelial sodium channel. *J Biol Chem, 284*(43), 29320-29325. doi: 10.1074/jbc.M109.046771

Condeelis, J., & Pollard, J. W. (2006). Macrophages: obligate partners for tumor cell migration, invasion, and metastasis. *Cell, 124*(2), 263-266. doi: 10.1016/j.cell.2006.01.007

Cooper, G. M., & Hausman, R. E. (2000). The development and causes of cancer. *The cell: A molecular approach*, 725-766.

Coronella, J. A., Telleman, P., Kingsbury, G. A., Truong, T. D., Hays, S., & Junghans, R. P. (2001). Evidence for an antigen-driven humoral immune response in medullary ductal breast cancer. *Cancer Res, 61*(21), 7889-7899.

Coussens, L. M., Fingleton, B., & Matrisian, L. M. (2002). Matrix metalloproteinase inhibitors and cancer: trials and tribulations. *Science, 295*(5564), 2387-2392. doi: 10.1126/science.1067100

Danhier, F., Feron, O., & Preat, V. (2010). To exploit the tumor microenvironment: Passive and active tumor targeting of nanocarriers for anti-cancer drug delivery. *J Control Release, 148*(2), 135-146. doi: 10.1016/j.jconrel.2010.08.027

Deshpande, P. P., Biswas, S., & Torchilin, V. P. (2013). Current trends in the use of liposomes for tumor targeting. *Nanomedicine (Lond), 8*(9), 1509-1528. doi: 10.2217/nnm.13.118

Dimasi, N., Fleming, R., Zhong, H., Bezabeh, B., Kinneer, K., Christie, R. J., . . . Gao, C. (2017). Efficient Preparation of Site-Specific Antibody-Drug Conjugates Using Cysteine Insertion. *Mol Pharm, 14*(5), 1501-1516. doi: 10.1021/acs.molpharmaceut.6b00995

Dranoff, G. (2004). Cytokines in cancer pathogenesis and cancer therapy. *Nat Rev Cancer, 4*(1), 11-22. doi: 10.1038/nrc1252

Du, H., Cui, C., Wang, L., Liu, H., & Cui, G. (2011). Novel tetrapeptide, RGDF, mediated tumor specific liposomal doxorubicin (DOX) preparations. *Mol Pharm, 8*(4), 1224-1232. doi: 10.1021/mp200039s

Erez, N., Truitt, M., Olson, P., Arron, S. T., & Hanahan, D. (2010). Cancer-Associated Fibroblasts Are Activated in Incipient Neoplasia to Orchestrate Tumor-Promoting Inflammation in an NF-kappaB-Dependent Manner. *Cancer Cell, 17*(2), 135-147. doi: 10.1016/j.ccr.2009.12.041

Estrada, S., Nycander, M., Hill, N. J., Craven, C. J., Waltho, J. P., & Bjork, I. (1998). The role of Gly-4 of human cystatin A (stefin A) in the binding of target proteinases. Characterization by kinetic and equilibrium methods of the interactions of cystatin A Gly-4 mutants with papain, cathepsin B, and cathepsin L. *Biochemistry, 37*(20), 7551-7560. doi: 10.1021/bi980026r

Gindy, M. E., & Prud'homme, R. K. (2009). Multifunctional nanoparticles for imaging, delivery and targeting in cancer therapy. *Expert Opin Drug Deliv, 6*(8), 865-878. doi: 10.1517/17425240902932908

Gitelman, H. J. (1988). *Aluminum and health: A critical review*: CRC Press.

Gocheva, V., Zeng, W., Ke, D., Klimstra, D., Reinheckel, T., Peters, C., . . . Joyce, J. A. (2006). Distinct roles for cysteine cathepsin genes in multistage tumorigenesis. *Genes Dev, 20*(5), 543-556. doi: 10.1101/gad.1407406

Goel, R., Shah, N., Visaria, R., Paciotti, G. F., & Bischof, J. C. (2009). Biodistribution of TNF-alpha-coated gold nanoparticles in an in vivo model system. *Nanomedicine (Lond), 4*(4), 401-410. doi: 10.2217/nnm.09.21

Goldenbogen, B., Brodersen, N., Gramatica, A., Loew, M., Liebscher, J., Herrmann, A., . . . Arbuzova, A. (2011). Reduction-sensitive liposomes from a multifunctional lipid conjugate and natural phospholipids: reduction and release kinetics and cellular uptake. *Langmuir, 27*(17), 10820-10829. doi: 10.1021/la201160y

Golos, A., & Lutynska, A. (2015). Aluminium-adjuvanted vaccines--a review of the current state of knowledge. *Przegl Epidemiol, 69*(4), 731-734, 871-734.

Gormley, J. A., Hegarty, S. M., O'Grady, A., Stevenson, M. R., Burden, R. E., Barrett, H. L., . . . Olwill, S. A. (2011). The role of Cathepsin S as a marker of prognosis and predictor of chemotherapy benefit in adjuvant CRC: a pilot study. *Br J Cancer, 105*(10), 1487-1494. doi: 10.1038/bjc.2011.408

Gosk, S., Moos, T., Gottstein, C., & Bendas, G. (2008). VCAM-1 directed immunoliposomes selectively target tumor vasculature in vivo. *Biochim Biophys Acta, 1778*(4), 854-863. doi: 10.1016/j.bbamem.2007.12.021

Greish, K. (2010). Enhanced permeability and retention (EPR) effect for anticancer nanomedicine drug targeting. *Methods Mol Biol, 624*, 25-37. doi: 10.1007/978-1-60761-609-2_3

Grull, H., & Langereis, S. (2012). Hyperthermia-triggered drug delivery from temperature-sensitive liposomes using MRI-guided high intensity focused ultrasound. *J Control Release, 161*(2), 317-327. doi: 10.1016/j.jconrel.2012.04.041

Guinec, N., Dalet-Fumeron, V., & Pagano, M. (1993). "In vitro" study of basement membrane degradation by the cysteine proteinases, cathepsins B, B-like and L. Digestion of collagen IV, laminin, fibronectin, and release of gelatinase activities from basement membrane fibronectin. *Biol Chem Hoppe Seyler, 374*(12), 1135-1146. doi: 10.1515/bchm3.1993.374.7-12.1135

Guncar, G., Pungercic, G., Klemencic, I., Turk, V., & Turk, D. (1999). Crystal structure of MHC class II-associated p41 Ii fragment bound to cathepsin L reveals the structural basis for differentiation between cathepsins L and S. *EMBO J, 18*(4), 793-803. doi: 10.1093/emboj/18.4.793

Guo, D., Zhao, Y., Zhang, Y., Wang, Q., Huang, Z., Ding, Q., . . . Gu, N. (2014). The cellular uptake and cytotoxic effect of silver nanoparticles on chronic myeloid leukemia cells. *J Biomed Nanotechnol, 10*(4), 669-678. doi: 10.1166/jbn.2014.1625

Gurunathan, S., Han, J. W., Eppakayala, V., Jeyaraj, M., & Kim, J. H. (2013). Cytotoxicity of biologically synthesized silver nanoparticles in MDA-MB-231 human breast cancer cells. *Biomed Res Int, 2013*, 535796. doi: 10.1155/2013/535796

Hamano, Y., Zeisberg, M., Sugimoto, H., Lively, J. C., Maeshima, Y., Yang, C., . . . Kalluri, R. (2003). Physiological levels of tumstatin, a fragment of collagen IV alpha3 chain, are generated by MMP-9 proteolysis and suppress angiogenesis via alphaV beta3 integrin. *Cancer Cell, 3*(6), 589-601.

Hanahan, D., & Weinberg, R. A. (2000). The hallmarks of cancer. *Cell, 100*(1), 57-70.

Hanahan, D., & Weinberg, R. A. (2011). Hallmarks of cancer: the next generation. *Cell, 144*(5), 646-674. doi: 10.1016/j.cell.2011.02.013

Hatakeyama, H., Akita, H., Ishida, E., Hashimoto, K., Kobayashi, H., Aoki, T., . . . Harashima, H. (2007). Tumor targeting of doxorubicin by anti-MT1-MMP antibody-modified PEG liposomes. *Int J Pharm, 342*(1-2), 194-200. doi: 10.1016/j.ijpharm.2007.04.037

Hilger, I., Hiergeist, R., Hergt, R., Winnefeld, K., Schubert, H., & Kaiser, W. A. (2002). Thermal ablation of tumors using magnetic nanoparticles: an in vivo feasibility study. *Invest Radiol, 37*(10), 580-586. doi: 10.1097/00004424-200210000-00008

Hiraoka, K., Miyazaki, H., Niisato, N., Iwasaki, Y., Kawauchi, A., Miki, T., & Marunaka, Y. (2010). Chloride ion modulates cell proliferation of human androgen-independent prostatic cancer cell. *Cell Physiol Biochem, 25*(4-5), 379-388. doi: 10.1159/000303042

Hoffmann, T., Stadler, L. K., Busby, M., Song, Q., Buxton, A. T., Wagner, S. D., . . . Ko Ferrigno, P. (2010). Structure-function studies of an engineered scaffold protein derived from stefin A. I: Development of the SQM variant. *Protein Eng Des Sel, 23*(5), 403-413. doi: 10.1093/protein/gzq012

Honey, K., Benlagha, K., Beers, C., Forbush, K., Teyton, L., Kleijmeer, M. J., . . . Bendelac, A. (2002). Thymocyte expression of cathepsin L is essential for NKT cell development. *Nat Immunol, 3*(11), 1069-1074. doi: 10.1038/ni844

Hood, J. D., & Cheresh, D. A. (2002). Role of integrins in cell invasion and migration. *Nat Rev Cancer, 2*(2), 91-100. doi: 10.1038/nrc727

Hsieh, C. S., deRoos, P., Honey, K., Beers, C., & Rudensky, A. Y. (2002). A role for cathepsin L and cathepsin S in peptide generation for MHC class II presentation. *J Immunol, 168*(6), 2618-2625. doi: 10.4049/jimmunol.168.6.2618

Jain, R. K. (2005). Normalization of tumor vasculature: an emerging concept in antiangiogenic therapy. *Science, 307*(5706), 58-62. doi: 10.1126/science.1104819

Jenko, S., Dolenc, I., Guncar, G., Dobersek, A., Podobnik, M., & Turk, D. (2003). Crystal structure of stefin A in complex with cathepsin H: N-terminal residues of inhibitors can adapt to the active sites of endo- and exopeptidases. *J Mol Biol, 326*(3), 875-885. doi: 10.1016/S0022-2836(02)01432-8

Jin, H., & Varner, J. (2004). Integrins: roles in cancer development and as treatment targets. *Br J Cancer, 90*(3), 561-565. doi: 10.1038/sj.bjc.6601576

Jordans, S., Jenko-Kokalj, S., Kuhl, N. M., Tedelind, S., Sendt, W., Bromme, D., . . . Brix, K. (2009). Monitoring compartment-specific substrate cleavage by cathepsins B, K, L, and S at physiological pH and redox conditions. *BMC Biochem, 10*, 23. doi: 10.1186/1471-2091-10-23

Joyce, J. A. (2005). Therapeutic targeting of the tumor microenvironment. *Cancer Cell, 7*(6), 513-520. doi: 10.1016/j.ccr.2005.05.024

Joyce, J. A., Baruch, A., Chehade, K., Meyer-Morse, N., Giraudo, E., Tsai, F. Y., . . . Hanahan, D. (2004). Cathepsin cysteine proteases are effectors of invasive growth and angiogenesis during multistage tumorigenesis. *Cancer Cell, 5*(5), 443-453.

Katanasaka, Y., Ida, T., Asai, T., Maeda, N., & Oku, N. (2008). Effective delivery of an angiogenesis inhibitor by neovessel-targeted liposomes. *Int J Pharm, 360*(1-2), 219-224. doi: 10.1016/j.ijpharm.2008.04.046

Kenig, S., Alonso, M. B., Mueller, M. M., & Lah, T. T. (2010). Glioblastoma and endothelial cells cross-talk, mediated by SDF-1, enhances tumour invasion and endothelial proliferation by increasing expression of cathepsins B, S, and MMP-9. *Cancer Lett, 289*(1), 53-61. doi: 10.1016/j.canlet.2009.07.014

Kim, S. K., & Huang, L. (2012). Nanoparticle delivery of a peptide targeting EGFR signaling. *J Control Release, 157*(2), 279-286. doi: 10.1016/j.jconrel.2011.08.014

Klasen, H. J. (2000). A historical review of the use of silver in the treatment of burns. II. Renewed interest for silver. *Burns, 26*(2), 131-138. doi: 10.1016/s0305-4179(99)00116-3

Koren, E., Apte, A., Jani, A., & Torchilin, V. P. (2012). Multifunctional PEGylated 2C5-immunoliposomes containing pH-sensitive bonds and TAT peptide for enhanced

tumor cell internalization and cytotoxicity. *J Control Release, 160*(2), 264-273. doi: 10.1016/j.jconrel.2011.12.002

Kos, J., Sekirnik, A., Kopitar, G., Cimerman, N., Kayser, K., Stremmer, A., . . . Werle, B. (2001). Cathepsin S in tumours, regional lymph nodes and sera of patients with lung cancer: relation to prognosis. *Br J Cancer, 85*(8), 1193-1200. doi: 10.1054/bjoc.2001.2057

Kramer, L., Renko, M., Zavrsnik, J., Turk, D., Seeger, M. A., Vasiljeva, O., . . . Turk, B. (2017). Non-invasive in vivo imaging of tumour-associated cathepsin B by a highly selective inhibitory DARPin. *Theranostics, 7*(11), 2806-2821. doi: 10.7150/thno.19081

Kramer, L., Turk, D., & Turk, B. (2017). The Future of Cysteine Cathepsins in Disease Management. *Trends Pharmacol Sci, 38*(10), 873-898. doi: 10.1016/j.tips.2017.06.003

Lah, T. T., Kokalj-Kunovar, M., Drobnic-Kosorok, M., Babnik, J., Golouh, R., Vrhovec, I., & Turk, V. (1992). Cystatins and cathepsins in breast carcinoma. *Biol Chem Hoppe Seyler, 373*(7), 595-604. doi: 10.1515/bchm3.1992.373.2.595

Lambert, J. M. (2013). Drug-conjugated antibodies for the treatment of cancer. *Br J Clin Pharmacol, 76*(2), 248-262. doi: 10.1111/bcp.12044

Ledakis, P., Tester, W. T., Rosenberg, N., Romero-Fischmann, D., Daskal, I., & Lah, T. T. (1996). Cathepsins D, B, and L in malignant human lung tissue. *Clin Cancer Res, 2*(3), 561-568.

Lee, H. J., Lee, Y. J., Kang, C. M., Bae, S., Jeoung, D., Jang, J. J., . . . Lee, Y. S. (2008). Differential gene signatures in rat mammary tumors induced by DMBA and those induced by fractionated gamma radiation. *Radiat Res, 170*(5), 579-590. doi: 10.1667/RR1106.1

Lee, R. J., & Low, P. S. (1995). Folate-mediated tumor cell targeting of liposome-entrapped doxorubicin in vitro. *Biochim Biophys Acta, 1233*(2), 134-144.

Lenarcic, B., Kos, J., Dolenc, I., Lucovnik, P., Krizaj, I., & Turk, V. (1988). Cathepsin D inactivates cysteine proteinase inhibitors, cystatins. *Biochem Biophys Res Commun, 154*(2), 765-772. doi: 10.1016/0006-291x(88)90206-9

Lerner, M. I., Mikhaylov, G., Tsukanov, A. A., Lozhkomoev, A. S., Gutmanas, E., Gotman, I., . . . Vasiljeva, O. (2018). Crumpled Aluminum Hydroxide Nanostructures as a Microenvironment Dysregulation Agent for Cancer Treatment. *Nano Lett, 18*(9), 5401-5410. doi: 10.1021/acs.nanolett.8b01592

Li, X., Ding, L., Xu, Y., Wang, Y., & Ping, Q. (2009). Targeted delivery of doxorubicin using stealth liposomes modified with transferrin. *Int J Pharm, 373*(1-2), 116-123. doi: 10.1016/j.ijpharm.2009.01.023

Li, Z., Hou, W. S., Escalante-Torres, C. R., Gelb, B. D., & Bromme, D. (2002). Collagenase activity of cathepsin K depends on complex formation with chondroitin sulfate. *J Biol Chem, 277*(32), 28669-28676. doi: 10.1074/jbc.M204004200

Li, Z., Yasuda, Y., Li, W., Bogyo, M., Katz, N., Gordon, R. E., . . . Bromme, D. (2004). Regulation of collagenase activities of human cathepsins by glycosaminoglycans. *J Biol Chem, 279*(7), 5470-5479. doi: 10.1074/jbc.M310349200

Libutti, S. K., Paciotti, G. F., Byrnes, A. A., Alexander, H. R., Jr., Gannon, W. E., Walker, M., . . . Tamarkin, L. (2010). Phase I and pharmacokinetic studies of CYT-6091, a novel PEGylated colloidal gold-rhTNF nanomedicine. *Clin Cancer Res, 16*(24), 6139-6149. doi: 10.1158/1078-0432.CCR-10-0978

Lin, E. Y., Li, J. F., Gnatovskiy, L., Deng, Y., Zhu, L., Grzesik, D. A., . . . Pollard, J. W. (2006). Macrophages regulate the angiogenic switch in a mouse model of breast cancer. *Cancer Res, 66*(23), 11238-11246. doi: 10.1158/0008-5472.CAN-06-1278

Marsh, T., Pietras, K., & McAllister, S. S. (2013). Fibroblasts as architects of cancer pathogenesis. *Biochim Biophys Acta, 1832*(7), 1070-1078. doi: 10.1016/j.bbadis.2012.10.013

Martinez-Jothar, L., Doulkeridou, S., Schiffelers, R. M., Sastre Torano, J., Oliveira, S., van Nostrum, C. F., & Hennink, W. E. (2018). Insights into maleimide-thiol conjugation chemistry: Conditions for efficient surface functionalization of nanoparticles for receptor targeting. *J Control Release, 282*, 101-109. doi: 10.1016/j.jconrel.2018.03.002

Mayle, K. M., Dern, K. R., Wong, V. K., Sung, S., Ding, K., Rodriguez, A. R., . . . Kamei, D. T. (2017). Polypeptide-Based Gold Nanoshells for Photothermal Therapy. *SLAS Technol, 22*(1), 18-25. doi: 10.1177/2211068216645292

Menard, R., Carmona, E., Takebe, S., Dufour, E., Plouffe, C., Mason, P., & Mort, J. S. (1998). Autocatalytic processing of recombinant human procathepsin L. Contribution of both intermolecular and unimolecular events in the processing of procathepsin L in vitro. *J Biol Chem, 273*(8), 4478-4484. doi: 10.1074/jbc.273.8.4478

Mihelic, M., Dobersek, A., Guncar, G., & Turk, D. (2008). Inhibitory fragment from the p41 form of invariant chain can regulate activity of cysteine cathepsins in antigen presentation. *J Biol Chem, 283*(21), 14453-14460. doi: 10.1074/jbc.M801283200

Mikhaylov, G., Klimpel, D., Schaschke, N., Mikac, U., Vizovisek, M., Fonovic, M., . . . Vasiljeva, O. (2014). Selective targeting of tumor and stromal cells by a nanocarrier system displaying lipidated cathepsin B inhibitor. *Angew Chem Int Ed Engl, 53*(38), 10077-10081. doi: 10.1002/anie.201402305

Mikhaylov, G., Mikac, U., Magaeva, A. A., Itin, V. I., Naiden, E. P., Psakhye, I., . . . Vasiljeva, O. (2011). Ferri-liposomes as an MRI-visible drug-delivery system for targeting tumours and their microenvironment. *Nat Nanotechnol, 6*(9), 594-602. doi: 10.1038/nnano.2011.112

Miyayama, T., & Matsuoka, M. (2016). Involvement of lysosomal dysfunction in silver nanoparticle-induced cellular damage in A549 human lung alveolar epithelial cells. *J Occup Med Toxicol, 11*, 1. doi: 10.1186/s12995-016-0090-0

Mosser, D. M., & Edwards, J. P. (2008). Exploring the full spectrum of macrophage activation. *Nat Rev Immunol, 8*(12), 958-969. doi: 10.1038/nri2448

Nakagawa, T., Roth, W., Wong, P., Nelson, A., Farr, A., Deussing, J., . . . Rudensky, A. Y. (1998). Cathepsin L: critical role in Ii degradation and CD4 T cell selection in the thymus. *Science, 280*(5362), 450-453. doi: 10.1126/science.280.5362.450

Nakamura, Y., Mochida, A., Choyke, P. L., & Kobayashi, H. (2016). Nanodrug Delivery: Is the Enhanced Permeability and Retention Effect Sufficient for Curing Cancer? *Bioconjug Chem, 27*(10), 2225-2238. doi: 10.1021/acs.bioconjchem.6b00437

Ngoune, R., Peters, A., von Elverfeldt, D., Winkler, K., & Putz, G. (2016). Accumulating nanoparticles by EPR: A route of no return. *J Control Release, 238*, 58-70. doi: 10.1016/j.jconrel.2016.07.028

Niedergethmann, M., Wostbrock, B., Sturm, J. W., Willeke, F., Post, S., & Hildenbrand, R. (2004). Prognostic impact of cysteine proteases cathepsin B and cathepsin L in pancreatic adenocarcinoma. *Pancreas, 29*(3), 204-211. doi: 10.1097/00006676-200410000-00005

Nishimura, Y., Kawabata, T., Furuno, K., & Kato, K. (1989). Evidence that aspartic proteinase is involved in the proteolytic processing event of procathepsin L in lysosomes. *Arch Biochem Biophys, 271*(2), 400-406. doi: 10.1016/0003-9861(89)90289-0

Obermajer, N., Repnik, U., Jevnikar, Z., Turk, B., Kreft, M., & Kos, J. (2008). Cysteine protease cathepsin X modulates immune response via activation of beta2 integrins. *Immunology, 124*(1), 76-88. doi: 10.1111/j.1365-2567.2007.02740.x

Olson, O. C., & Joyce, J. A. (2015). Cysteine cathepsin proteases: regulators of cancer progression and therapeutic response. *Nat Rev Cancer, 15*(12), 712-729. doi: 10.1038/nrc4027

Panzarini, E., Inguscio, V., Tenuzzo, B. A., Carata, E., & Dini, L. (2013). Nanomaterials and autophagy: new insights in cancer treatment. *Cancers (Basel), 5*(1), 296-319. doi: 10.3390/cancers5010296

Papetti, M., & Herman, I. M. (2002). Mechanisms of normal and tumor-derived angiogenesis. *Am J Physiol Cell Physiol, 282*(5), C947-970. doi: 10.1152/ajpcell.00389.2001

Paszko, E., & Senge, M. O. (2012). Immunoliposomes. *Curr Med Chem, 19*(31), 5239-5277. doi: 10.2174/092986712803833362

Pavlova, A., & Bjork, I. (2002). The role of the second binding loop of the cysteine protease inhibitor, cystatin A (stefin A), in stabilizing complexes with target proteases is exerted predominantly by Leu73. *Eur J Biochem, 269*(22), 5649-5658. doi: 10.1046/j.1432-1033.2002.03273.x

Puri, A., Loomis, K., Smith, B., Lee, J. H., Yavlovich, A., Heldman, E., & Blumenthal, R. (2009). Lipid-based nanoparticles as pharmaceutical drug carriers: from concepts to clinic. *Crit Rev Ther Drug Carrier Syst, 26*(6), 523-580.

Quail, D. F., & Joyce, J. A. (2013). Microenvironmental regulation of tumor progression and metastasis. *Nat Med, 19*(11), 1423-1437. doi: 10.1038/nm.3394

Reinheckel, T., Hagemann, S., Dollwet-Mack, S., Martinez, E., Lohmuller, T., Zlatkovic, G., . . . Peters, C. (2005). The lysosomal cysteine protease cathepsin L regulates keratinocyte proliferation by control of growth factor recycling. *J Cell Sci, 118*(Pt 15), 3387-3395. doi: 10.1242/jcs.02469

Renko, M., Pozgan, U., Majera, D., & Turk, D. (2010). Stefin A displaces the occluding loop of cathepsin B only by as much as required to bind to the active site cleft. *FEBS J, 277*(20), 4338-4345. doi: 10.1111/j.1742-4658.2010.07824.x

Rousselet, N., Mills, L., Jean, D., Tellez, C., Bar-Eli, M., & Frade, R. (2004). Inhibition of tumorigenicity and metastasis of human melanoma cells by anti-cathepsin L single chain variable fragment. *Cancer Res, 64*(1), 146-151.

Semenza, G. L. (2013). Cancer-stromal cell interactions mediated by hypoxia-inducible factors promote angiogenesis, lymphangiogenesis, and metastasis. *Oncogene, 32*(35), 4057-4063. doi: 10.1038/onc.2012.578

Sevenich, L., Bowman, R. L., Mason, S. D., Quail, D. F., Rapaport, F., Elie, B. T., . . . Joyce, J. A. (2014). Analysis of tumour- and stroma-supplied proteolytic networks reveals a brain-metastasis-promoting role for cathepsin S. *Nat Cell Biol, 16*(9), 876-888. doi: 10.1038/ncb3011

Shalapour, S., & Karin, M. (2015). Immunity, inflammation, and cancer: an eternal fight between good and evil. *J Clin Invest, 125*(9), 3347-3355. doi: 10.1172/JCI80007

Shen, B. Q., Xu, K., Liu, L., Raab, H., Bhakta, S., Kenrick, M., . . . Junutula, J. R. (2012). Conjugation site modulates the in vivo stability and therapeutic activity of antibody-drug conjugates. *Nat Biotechnol, 30*(2), 184-189. doi: 10.1038/nbt.2108

Shmeeda, H., Tzemach, D., Mak, L., & Gabizon, A. (2009). Her2-targeted pegylated liposomal doxorubicin: retention of target-specific binding and cytotoxicity after in vivo passage. *J Control Release, 136*(2), 155-160. doi: 10.1016/j.jconrel.2009.02.002

Shree, T., Olson, O. C., Elie, B. T., Kester, J. C., Garfall, A. L., Simpson, K., . . . Joyce, J. A. (2011). Macrophages and cathepsin proteases blunt chemotherapeutic response in breast cancer. *Genes Dev, 25*(23), 2465-2479. doi: 10.1101/gad.180331.111

Sobotic, B., Vizovisek, M., Vidmar, R., Van Damme, P., Gocheva, V., Joyce, J. A., . . . Fonovic, M. (2015). Proteomic Identification of Cysteine Cathepsin Substrates Shed from the Surface of Cancer Cells. *Mol Cell Proteomics, 14*(8), 2213-2228. doi: 10.1074/mcp.M114.044628

Som, A., Raliya, R., Tian, L., Akers, W., Ippolito, J. E., Singamaneni, S., . . . Achilefu, S. (2016). Monodispersed calcium carbonate nanoparticles modulate local pH and inhibit tumor growth in vivo. *Nanoscale, 8*(25), 12639-12647. doi: 10.1039/c5nr06162h

Stadler, L. K., Hoffmann, T., Tomlinson, D. C., Song, Q., Lee, T., Busby, M., . . . Ferrigno, P. K. (2011). Structure-function studies of an engineered scaffold protein derived from Stefin A. II: Development and applications of the SQT variant. *Protein Eng Des Sel, 24*(9), 751-763. doi: 10.1093/protein/gzr019

Strojnik, T., Kavalar, R., Trinkaus, M., & Lah, T. T. (2005). Cathepsin L in glioma progression: comparison with cathepsin B. *Cancer Detect Prev, 29*(5), 448-455. doi: 10.1016/j.cdp.2005.07.006

Stubbs, M., McSheehy, P. M., Griffiths, J. R., & Bashford, C. L. (2000). Causes and consequences of tumour acidity and implications for treatment. *Mol Med Today, 6*(1), 15-19. doi: 10.1016/s1357-4310(99)01615-9

Tachibana, T., Onodera, H., Tsuruyama, T., Mori, A., Nagayama, S., Hiai, H., & Imamura, M. (2005). Increased intratumor Valpha24-positive natural killer T

cells: a prognostic factor for primary colorectal carcinomas. *Clin Cancer Res, 11*(20), 7322-7327. doi: 10.1158/1078-0432.CCR-05-0877

Talmadge, J. E., & Gabrilovich, D. I. (2013). History of myeloid-derived suppressor cells. *Nat Rev Cancer, 13*(10), 739-752. doi: 10.1038/nrc3581

Tanada, S., Kabayama, M., Kawasaki, N., Sakiyama, T., Nakamura, T., Araki, M., & Tamura, T. (2003). Removal of phosphate by aluminum oxide hydroxide. *J Colloid Interface Sci, 257*(1), 135-140. doi: 10.1016/s0021-9797(02)00008-5

Thomssen, C., Schmitt, M., Goretzki, L., Oppelt, P., Pache, L., Dettmar, P., . . . Graeff, H. (1995). Prognostic value of the cysteine proteases cathepsins B and cathepsin L in human breast cancer. *Clin Cancer Res, 1*(7), 741-746.

Torchilin, V. (2009). Multifunctional and stimuli-sensitive pharmaceutical nanocarriers. *Eur J Pharm Biopharm, 71*(3), 431-444. doi: 10.1016/j.ejpb.2008.09.026

Tran, S., DeGiovanni, P. J., Piel, B., & Rai, P. (2017). Cancer nanomedicine: a review of recent success in drug delivery. *Clin Transl Med, 6*(1), 44. doi: 10.1186/s40169-017-0175-0

Turk, B. (2006). Targeting proteases: successes, failures and future prospects. *Nat Rev Drug Discov, 5*(9), 785-799. doi: 10.1038/nrd2092

Turk, V., & Bode, W. (1994). 4 Human Cysteine Proteinases and Their Inhibitors, Stefins and Cystatins *Biological functions of proteases and inhibitors* (pp. 47-59): Karger Publishers.

Turk, V., Stoka, V., Vasiljeva, O., Renko, M., Sun, T., Turk, B., & Turk, D. (2012). Cysteine cathepsins: from structure, function and regulation to new frontiers. *Biochim Biophys Acta, 1824*(1), 68-88. doi: 10.1016/j.bbapap.2011.10.002

Urbich, C., Heeschen, C., Aicher, A., Sasaki, K., Bruhl, T., Farhadi, M. R., . . . Dimmeler, S. (2005). Cathepsin L is required for endothelial progenitor cell-induced neovascularization. *Nat Med, 11*(2), 206-213. doi: 10.1038/nm1182

Vasiljeva, O., Papazoglou, A., Kruger, A., Brodoefel, H., Korovin, M., Deussing, J., . . . Reinheckel, T. (2006). Tumor cell-derived and macrophage-derived cathepsin B promotes progression and lung metastasis of mammary cancer. *Cancer Res, 66*(10), 5242-5250. doi: 10.1158/0008-5472.CAN-05-4463

Veillard, F., Saidi, A., Burden, R. E., Scott, C. J., Gillet, L., Lecaille, F., & Lalmanach, G. (2011). Cysteine cathepsins S and L modulate anti-angiogenic activities of human endostatin. *J Biol Chem, 286*(43), 37158-37167. doi: 10.1074/jbc.M111.284869

Wang, B., Sun, J., Kitamoto, S., Yang, M., Grubb, A., Chapman, H. A., . . . Shi, G. P. (2006). Cathepsin S controls angiogenesis and tumor growth via matrix-derived angiogenic factors. *J Biol Chem, 281*(9), 6020-6029. doi: 10.1074/jbc.M509134200

Wang, F., Salvati, A., & Boya, P. (2018). Lysosome-dependent cell death and deregulated autophagy induced by amine-modified polystyrene nanoparticles. *Open Biol, 8*(4). doi: 10.1098/rsob.170271

Watanabe, K., Kaneko, M., & Maitani, Y. (2012). Functional coating of liposomes using a folate- polymer conjugate to target folate receptors. *Int J Nanomedicine, 7*, 3679-3688. doi: 10.2147/IJN.S32853

Wicki, A., Witzigmann, D., Balasubramanian, V., & Huwyler, J. (2015). Nanomedicine in cancer therapy: challenges, opportunities, and clinical applications. *J Control Release, 200*, 138-157. doi: 10.1016/j.jconrel.2014.12.030

Woodman, R., Yeh, J. T., Laurenson, S., & Ko Ferrigno, P. (2005). Design and validation of a neutral protein scaffold for the presentation of peptide aptamers. *J Mol Biol, 352*(5), 1118-1133. doi: 10.1016/j.jmb.2005.08.001

Yang, Z., & Cox, J. L. (2007). Cathepsin L increases invasion and migration of B16 melanoma. *Cancer Cell Int, 7*(1), 8. doi: 10.1186/1475-2867-7-8

Yildirim, S., Altun, S., Gumushan, H., Patel, A., & Djamgoz, M. B. A. (2012). Voltage-gated sodium channel activity promotes prostate cancer metastasis in vivo. *Cancer Lett, 323*(1), 58-61. doi: 10.1016/j.canlet.2012.03.036

Zhai, G., Wu, J., Yu, B., Guo, C., Yang, X., & Lee, R. J. (2010). A transferrin receptor-targeted liposomal formulation for docetaxel. *J Nanosci Nanotechnol, 10*(8), 5129-5136.

Zhao, W., Zhuang, S., & Qi, X. R. (2011). Comparative study of the in vitro and in vivo characteristics of cationic and neutral liposomes. *Int J Nanomedicine, 6*, 3087-3098. doi: 10.2147/IJN.S25399

Bibliography

Publications Related to the Thesis

Journal Articles

Bratovš, A., Kramer, L., Mikhaylov, G., Vasiljeva, O., & Turk, B. (2019). Stefin A-functionalized liposomes as a system for cathepsins S and L-targeted drug delivery. Biochimie, 166, 94-102. doi: 10.1016/j.biochi.2019.05.018

Lerner, M. I., Mikhaylov, G., Tsukanov, A. A., Lozhkomoev, A. S., Gutmanas, E., Gotman, I., . . . Vasiljeva, O. (2018). Crumpled Aluminum Hydroxide Nanostructures as a Microenvironment Dysregulation Agent for Cancer Treatment. Nano Lett, 18(9), 5401-5410. doi: 10.1021/acs.nanolett.8b01592

Vizovišek, M., Vidak, E., Javorsek, U., Mikhaylov, G., Bratovš, A., & Turk, B. (2020). Cysteine cathepsins as therapeutic targets in inflammatory diseases. Expert Opin Ther Targets, 2020, 1-16. doi: 10.1080/14728222.2020.1746765

Conference Papers

Bratovš, A., Kramer, L., Mikhaylov, G., Vasiljeva, O., Turk, B. Stefin A-functionalized liposomes as a system for cathepsins S and L-targeted drug delivery. In *11th General Meeting of the International Proteolysis Society, 'Interfaces in Proteolysis'*, 29 Sep - 4 Oct 2019, Mariánské Lázně, Czech Republic.

Mikhaylov, G., Bratovš, A., Turk, V., Turk, B., Vasiljeva, O. Anticancer activity of crumpled aluminum nanosheets through disruption of ion balance in tumor microenvironment. In *8th International Workshop "Multiscale biomechanics and tribology of inorganic and Organic Systems"*, 1-5 October 2019, Tomsk, Russia.

Bratovš, A., Kramer, L., Mikhaylov, G., Vasiljeva, O., Turk, B. Stefin A-functionalized liposomes as a system for cathepsins S and L-targeted drug delivery. *In Book of abstracts. 6th Conference on Mitochondria, Apoptosis and Cancer (MAC'19)*, September 17-20, 2019, Prague, Czech Republic,.

Bratovš, A., Kramer, L., Mikhaylov, G., Vasiljeva, O., Turk, B. Stefin A as a ligand for cathepsins S and L-targeted drug delivery. In *16. International Symposium on Proteases, Inhibitors and Biological Control*, 08. 09.-12. 09. 2018, Portorož, Slovenia.

Bratovš, A., Kramer, L., Vasiljeva, O., Turk, B. Stefin A as a ligand cathepsins S and L-targeted drug delivery. In *XXXVth Winter School on Proteinases and Their Inhibitors*, February 28th - March 4th, 2018, Tiers am Rosengarten, Italy.

Bratovš, A., Kramer, L., Vasiljeva, O., Turk, B. Targeting cathepsins B, S and L with DARPin/stefinA-conjugated liposomes in cancer. In *Mitochondria, apoptosis and cancer*, 16. 09.-18. 09. 2017, Bled, Slovenia.

Biography

Andreja Bratovš obtained her Master's Degree in Biochemistry in September 2015 at the Faculty of Chemistry and Chemical Technology, University of Ljubljana. In October 2015, she enrolled in the Nanosciences and nanotechnologies programme at the Jožef Stefan International Postgraduate School under the supervision of Prof. Dr. Olga Vasiljeva and co-supervision of Prof. DDr. Boris Turk. At the same time, she started working as a young researcher at the Jožef Stefan Institute at the Department of Biochemistry, Molecular and Structural Biology.